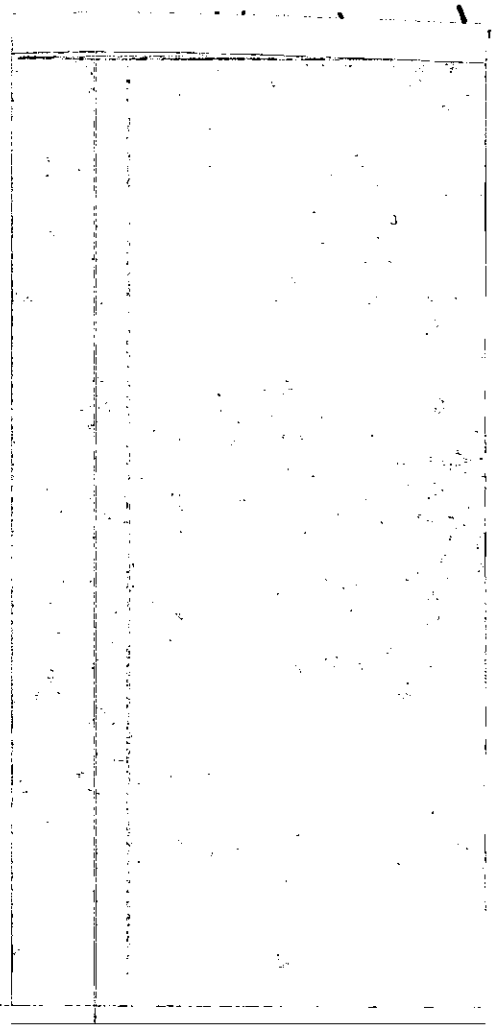


"In presenting the dissertation as a partial fulfillment of the requirements for an advanced degree from the Georgia Institute of Technology, I agree that the Library of the Institution shall make it available for inspection and circulation in accordance with its regulations governing materials of this type. I agree that permission to copy from, or to publish from, this dissertation may be granted by the professor under whose direction it was written, or, in his absence, by the dean of the Graduate Division when such copying or publication is solely for scholarly purposes and does not involve potential financial gain. It is understood that any copying from, or publication of, this dissertation which involves potential financial gain will not be allowed without written permission.



THE ELECTRONIC SPECTRUM OF  
DECABORANE AND ITS DERIVATIVES

A THESIS

Presented to  
the Faculty of the Graduate Division  
by  
Arne Haaland

In Partial Fulfillment  
of the Requirements for the Degree  
Doctor of Philosophy in the School  
of Chemistry

Georgia Institute of Technology

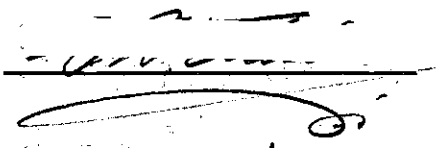
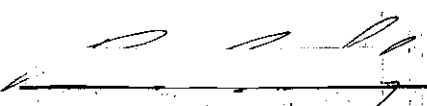
August, 1961



5 A  
12T

THE ELECTRONIC SPECTRUM OF  
DECABORANE AND ITS DERIVATIVES

APPROVED:

  
\_\_\_\_\_  
  
\_\_\_\_\_

Date Approved by Chairman : August 18, 1961

## ACKNOWLEDGEMENTS

The author wishes to thank Dr. W. H. Eberhardt for his kind help, advice, and understanding over the last three years, and Dr. P. B. Sherry and Dr. T. L. Weatherly for serving on his reading committee.

He is grateful to the Alfred P. Sloan Foundation and the Georgia Tech World Student Fund for financial assistance.

Finally, he would like to thank the innumerable individuals at Georgia Tech and in Atlanta that have made his stay in the United States a memorable experience.

## TABLE OF CONTENTS

	Page
ACKNOWLEDGEMENTS . . . . .	ii
LIST OF TABLES . . . . .	iv
LIST OF ILLUSTRATIONS. . . . .	v
LIST OF SYMBOLS. . . . .	vi
SUMMARY. . . . .	viii
Chapter	
I. INTRODUCTION. . . . .	1
General . . . . .	1
Theories of Bonding in Decaborane . . . . .	6
II. EXPERIMENTAL. . . . .	15
Solution Spectra. . . . .	16
Gas Spectrum. . . . .	17
Crystal Spectra . . . . .	18
Glass Spectrum. . . . .	27
III. A REVIEW OF THE THEORY OF ELECTRONIC SPECTRA OF MOLECULAR CRYSTALS. . . . .	28
IV. RESULTS AND DISCUSSION. . . . .	49
Solution Spectra. . . . .	49
Gas Spectrum. . . . .	51
Glass Spectrum. . . . .	51
Crystal Spectra . . . . .	52
Concluding Remarks. . . . .	71
V. CONCLUSIONS AND RECOMMENDATIONS . . . . .	73
Appendix	
ON THE CHEMISTRY OF DECABORANE . . . . .	76
BIBLIOGRAPHY . . . . .	77
VITA . . . . .	82

## LIST OF TABLES

Table		Page
1.	The Known Boranes and their Physical Constants. . . . .	2
2.	Absorption Spectra of Solutions of $B_{10}H_{14}$ and $2,4-B_{10}H_{12}I_2$ at $25^{\circ}C$ . . . . .	50
3.	Absorption Lines of Radiation Polarized along the b-Axis of Monocrystalline Decaborane at $4.2^{\circ}K$ . . . . .	53
4.	The Character Tables of the Molecular Point Group, the Site Group, and the Factor Group of Decaborane. . . . .	57
5.	Relations between Molecular and Crystal States of Decaborane. . . . .	62

## LIST OF ILLUSTRATIONS

Figure		Page
1.	Molecular Structure of Decaborane. . . . .	4
2.	The Liquid Helium Cryostat . . . . .	23
3.	Absorption of Radiation Polarized along the b-Axis of Monocrystalline Decaborane at 4.2°K . . . . .	54
4.	Crystal Structure of Decaborane. . . . .	56
5.	Vibrational Structure of the Spectrum of Crystalline Decaborane . . . . .	68

## LIST OF SYMBOLS

I. The Free Molecule

M		The molecular point group
h		Hamiltonian
$\varphi^{(0)}$	$w^{(0)}$	Wavefunction and energy of the ground state
$\varphi^{(i)}$	$w^{(i)}$	Wavefunction and energy of an excited state

II. The Molecule in the Crystal

S		The site group
s		The order of the site group
h'		Hamiltonian of the molecule
$\varphi^0$	$w^0$	Wavefunction and energy of the ground state
$\varphi^i$	$w^i$	Wavefunction and energy of an excited state
i		The irreducible representation of S to which $\varphi^i$ belongs

III. The Crystal

$N^3$		Number of unit cells in the crystal
n		Number of molecules in the unit cell
ab,cd,kl		Indices denoting unit cell (a,c,d) and site in unit cell (b,d,l)
G		The space group
g		The order of the space group
R		A symmetry operation
T		The group of primitive translations
t		A primitive translation



F	The factor group
f	The order of the factor group
TR	An element of F
tR	An element in TR
H	The crystal Hamiltonian
V	The interaction potential
$\Psi^0$	The wavefunction of the ground state of the crystal
$\Phi_{kl}^i$	A one-molecule exciton: $\Phi_{kl}^i = \Phi_{kl}^i \prod_a \prod_b' \Phi_{ab}^0$
$\underline{K}$	A vector to a point inside the unit cell of the reciprocal lattice: The wavevector
$\psi_1^i(\underline{K})$	A one-site exciton on site 1 characterized by the wavevector $\underline{K}$
$\Psi^j$	The wavefunction of an excited state of the crystal
j	The irreducible representation of F to which $\Psi^j$ belongs
C	The matrix element of H between two one-site excitons with wavevector zero:

$$C = (\psi_b^i(\underline{0}) \mid H \mid \psi_d^i(\underline{0}))$$

## SUMMARY

The near ultraviolet absorption spectrum of gaseous, dissolved, and crystalline decaborane is investigated.

Evidence is found for only one transition of energy less than 5.0 ev, the energy of the 0-0 transition being 3.85 ev. The transition moment,  $p$ , and oscillator strength,  $f$ , were determined from the absorption spectrum of decaborane in cyclohexane solution:

$$p^2 = 0.21 \times 10^{-16} \text{ cm}^2 \text{ and } f = 0.10$$

The solvent effect indicates that the dipole moment of the excited state is less than the dipole moment of the ground state.

The absorption of polarized radiation by monocrystals at 4.2° K was measured using a liquid helium cryostat that is described, and the results clearly indicate that the excited molecular state is of symmetry  $B_1$  or  $B_2$ . The transition is therefore allowed for radiation polarized perpendicular to the two-fold rotation axis of the molecule.

The effects of the crystal field on the spectrum are considered in detail. The decaborane crystal is somewhat anomalous in that it contains two sets of equivalent sites, as well as being highly twinned, and the theory is extended to take this into account. It is found that the crystal field induced splitting of vibronic levels should be insignificant, and none is found in the spectrum.

In the crystal the transition is accompanied by three vibrations of the excited molecule, the frequencies being:

$$\nu_1 = 425 \text{ cm}^{-1}$$

$$\nu_2 = 390 \text{ cm}^{-1}$$

$$\nu_3 = 135 \text{ cm}^{-1}$$

Some of the more important theories of bonding in decaborane (the Eberhardt, Crawford, and Lipscomb three-center bonds; completely delocalized bonds as calculated by Moore, Lohr, and Lipscomb; and the free particle in a hemispherical box approach) are examined. While none of the theories is in perfect agreement with the experimental results, they all predict correctly the symmetry of the wavefunction of the excited state, so this investigation does not rule out any of the three theories.

## CHAPTER I

### INTRODUCTION

General.--The history of the boron hydrides, or boranes, in chemistry is a short one. The boron-hydrogen bond is easily disrupted by water, and boron's affinity for oxygen is so great that in nature it is invariably found as boric acid or its salts. Elemental boron was first produced in 1808 by Gay-Lussac and Thenard (1) who heated boric acid with potassium and obtained a greenish brown, tasteless substance they called boron.

When boric acid is heated with an excess of magnesium, a mixture of boron and magnesium boride is obtained. Several early workers (2,3) investigated the reaction of this mixture with dilute acids. A gas was evolved that had a disagreeable odor, burned with a green flame, and precipitated metallic silver from silver salt solutions. Elemental analysis showed that the gas consisted of boron and hydrogen, but no one succeeded in establishing the formula.

It remained for Stock and his collaborators (4) to elucidate the nature of the gas. By repeated fractional distillation at low temperatures they showed that it is in fact a mixture of several boron-hydrogen compounds, and they succeeded in isolating and purifying no less than six components, the first, tetraborane, in 1912. The formulas were then established by molecular weight determination and elemental analysis. Many years later Schaeffer (5) isolated an enneaborane, bringing the number of known boranes up to seven. These are listed with their physical constants in Table 1.

Table 1. The Known Boranes and their Physical Constants. (6).

		m.p.	b.p.
diborane	$B_2H_6$	$-165.5^{\circ}C$	$-92.5^{\circ}C$
tetraborane	$B_4H_{10}$	$-120^{\circ}$	$-18^{\circ}$
pentaborane-9	$B_5H_9$	$-46.6^{\circ}$	$48^{\circ}$
pentaborane-11	$B_5H_{11}$	$-123^{\circ}$	$63^{\circ}$
hexaborane	$B_6H_{10}$	$-65^{\circ}$	
enneaborane	$B_9H_{15}$	$-20^{\circ}$	
decaborane	$B_{10}H_{14}$	$99.7^{\circ}$	$213^{\circ}$

All these compounds proved baffling to theoretical chemists. Their low melting and boiling points indicate that they are covalently bonded, and yet the valence rule that works so well for hydrocarbons and derivatives, namely that a bond is formed when two atoms share an electron pair, is violated. An example will make this clear: Each boron atom has three valence electrons, and each hydrogen atom has one. Diborane thus has  $2 \times 3 + 6 \times 1 = 12$  bonding electrons. If each hydrogen atom is bonded to a boron atom by a normal covalent bond,  $6 \times 2 = 12$  electrons will be required, and none will be left for a boron-boron bond. A similar deficit is found in the higher boranes, and they are therefore described as "electron-deficient" compounds. Stock (7) has reviewed most of the early theories of bonding in boranes, but since the molecular structures were unknown, these were all purely speculative.

The first member to be elucidated was the simplest, diborane (8). It was found to have two boron atoms and four hydrogen atoms in an ethylene-

like arrangement, with the two remaining hydrogen atoms between the boron atoms, the line connecting them perpendicular to the plane of the ethylene-like unit. This indicates that each of the two hydrogen atoms is bonded to two boron atoms in complete contradiction to the usual ideas of bonding of hydrogen atoms, and that the molecule contains a total of  $2 \times 4 = 8$  boron-hydrogen bonds which makes the "electron-deficiency" more acute than ever.

The structure of decaborane was determined by Kasper, Lucht, and Harker (9) in 1950 (Fig. 1). The ten boron atoms were found to occupy ten corners of a nearly regular icosahedron. This boron skeleton with the conventional numbering of the atoms is shown projected into the plane in Fig. 1B. Ten of the fourteen hydrogen atoms are bonded one to each boron atom by an external radial bond, and the remaining four occupy positions between boron atoms 5 and 6, 6 and 7, 8 and 9, and 9 and 10. The molecule has a two-fold axis of symmetry,  $C_2$ , and two mirror planes,  $\sigma_x$  and  $\sigma_y$ , all vertical to the plane of the paper in Fig. 1B. The molecular symmetry is thus  $C_{2v}$ . For future reference we define three molecular axes  $x$ ,  $y$ , and  $z$  as shown.

Instead of easing the electron deficiency, this structure appears to make it acute. Let us for instance regard boron atom 2. It has six near neighbors: boron atoms 1, 3, 5, 6, and 7 and one hydrogen atom, and should therefore be expected to form six bonds with only three valence electrons! Before the various theories of bonding in decaborane are examined, some of the chemical and physical evidence that might throw light on the problem will be summarized.

The x-ray structure of Kasper, Lucht, and Harker has been refined by Moore, Dickerson, and Lipscomb (10). The electron diffraction patterns observed by Silbiger and Bauer (11) were re-examined by Lucht (12) who

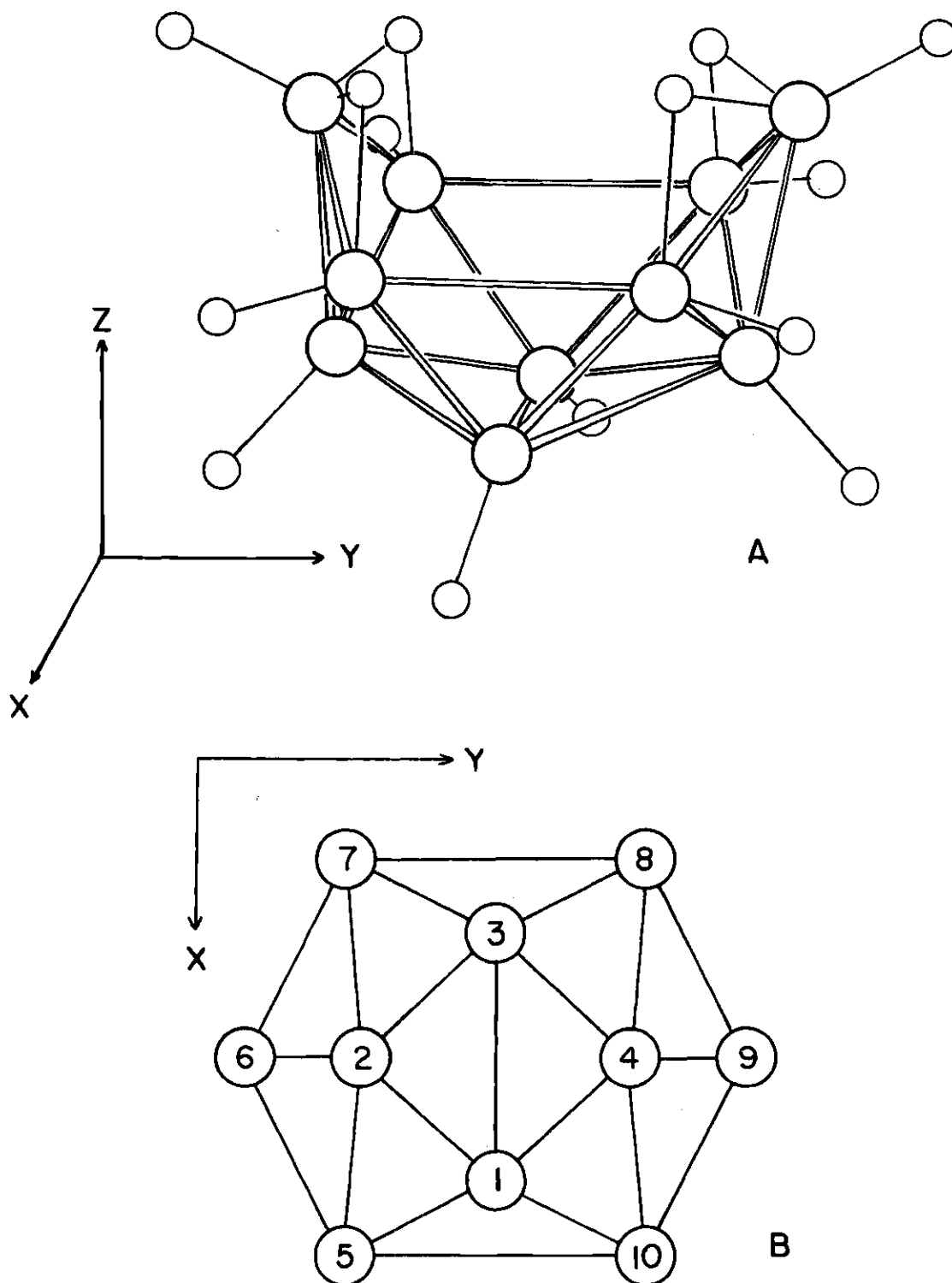
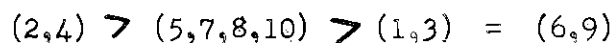


Figure 1. Molecular Structure of Decaborane (A). The Boron Framework Projected into the Plane (B).

found them to be in excellent agreement with the KLH model.

The dipole moment was measured in solution in benzene by Laubengayer and Bottei (13), and was found to have the surprisingly high value of  $3.52 \pm 0.02$  Debye. This large value is particularly surprising when it is remembered that the electronegativities of boron and hydrogen are nearly identical. The direction of the dipole moment is indicated by the  $B^{11}$  NMR spectrum (14, 15) which consists of a high field doublet and a low field triplet, the latter with intensity ratio 1:2:1. The high field doublet is accredited to boron atoms 2 and 4, the splitting being due to the external hydrogen atoms. The triplet consists of two partially overlapping doublets, one on the high field side due to 5, 7, 8 and 10 and one on the low field side due to accidental overlap of 1, 3, and 6, 9. Assuming that variations in shielding may be ascribed entirely to changes in electron density, the sites may be arranged in order of decreasing electron density:

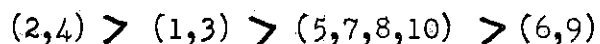


It seems surprising that sites 2, 4 and 1, 3 can be so different, and chemical evidence does indeed suggest that these sites are of more equal electron density than shown above.

Williams and coworkers (16) have examined the reaction of decaborane with several nucleophilic and electrophilic reagents. They found for instance that decaborane and methylbromide in the presence of aluminum chloride led to substitution of methyl first at the 2, then at the 1 and finally at the 5 position. Treatment with methyl-lithium on the other hand leads to substitution at the 6 and 9 positions and then slowly at



the 5 position. This indicates the following order of electron density:



This sequence is further supported by iodination studies (17), deuteration studies (18, 19), and the reaction of decaborane with electron donors like  $\text{CH}_3\text{CN}$  (20, 21, 22) and appears more likely than the one indicated by the NMR spectrum.

The infrared spectrum of crystalline decaborane and the Raman spectrum in solution in carbon disulfide have been measured from  $230\text{ cm}^{-1}$  to  $2700\text{ cm}^{-1}$  (23), but no normal coordinate treatment has been reported. Normal modes involving motions of hydrogen atoms are expected to have frequencies higher than  $800\text{ cm}^{-1}$  (24), so lower frequencies must be due to motions in the boron skeleton.

Pimentel and Pitzer (25) studied the ultraviolet absorption spectrum of decaborane in cyclohexane solution and found a single broad band beginning at  $3600\text{ \AA}$  with maximum at  $2720\text{ \AA}$ . The luminescence spectrum in isopentane-methylcyclopentane glass at  $77^\circ\text{K}$  was found to begin at  $3600\text{ \AA}$ , extending towards longer wavelengths. They therefore concluded that the 0-0 transition must be at  $3600 \pm 50\text{ \AA}$ .

The ionization potential by electron impact has been reported as  $11.0 \pm 0.5\text{ ev}$  (26).

Theories of Bonding in Decaborane.--Since it has been shown that the conventional two-center electron pair bond model fails to explain the structure of the boron hydrides, it is appropriate to review some of the more important theories of bonding in these compounds, particularly in decaborane.

Since one cannot localize the electrons in two-center orbitals, the logical view might be to consider orbitals extending over the entire molecule. This is certainly the correct procedure since even in hydrocarbons the localized bond is only an approximation. But by doing this one loses the simple picture of a chemical bond and all that this concept implies.

Some calculations also indicate that it is unnecessary to delocalize the electrons completely. Yamazaki (27) has carried out a detailed self-consistent-field linear-combination-of-atomic-orbitals (SCF LCAO) molecular-orbital calculation of diborane neglecting only the 1s electrons on the boron atoms. Hamilton (28) on the other hand assumed that the four equivalent hydrogen atoms are bonded to the boron atoms by simple two-center electron-pair bonds and thus considered the remaining four-center, four-electron problem. This approach gave an electron distribution nearly equal to that obtained by Yamazaki as indicated by a calculated overlap of 0.94 between the wavefunctions for the ground state proposed by the two workers. Complete agreement would, of course, give an overlap of 1.00.

The view of the four boron hydrogen bonds as localized is also well supported by chemical evidence. The hydrogens have been replaced by other groups as, for instance, alkyls (29), without significant change of molecular structure. The same holds true for decaborane; the ten external hydrogen atoms can be replaced by other groups without change in the molecular geometry. It has, therefore, been generally assumed that the bonds between the boron atoms and ten external hydrogens are simple single bonds. This leaves a 14-center 24-electron system.

Hamilton (30), using Yamazaki's data, was later able to write down two three-center orbitals for the  $B_2H_2$  system in diborane described above. Each of these orbitals involved the two boron atoms and one hydrogen atom, and constitutes what is called a hydrogen bridge bond. Using these orbitals the overlap with Yamazaki's ground state wavefunction becomes 0.998.

Before Hamilton's calculations Eberhardt, Crawford and Lipscomb (ECL)(31) had systematically explained the structures of the boron hydrides using only two- and three-center bonds. The two-center bond corresponds to a conventional chemical bond between two atoms. A bonding (b) electronic orbital is formed from two overlapping atomic orbitals  $\lambda_1$  and  $\lambda_2$ , one on each atom;

$$v_1 = 2^{-\frac{1}{2}} (\lambda_1 + \lambda_2) \quad (b) \quad (1.1)$$

The two atomic orbitals also combine to form an antibonding (ab) orbital,

$$v_2 = 2^{-\frac{1}{2}} (\lambda_1 - \lambda_2) \quad (ab) \quad (1.2)$$

and the energy difference between the two orbitals is  $2\beta$  where  $\beta$  is the exchange integral.

$$\beta = \int \lambda_1 h_{el} \lambda_2 d\tau \quad (1.3)$$

where  $h_{el}$  is the Hamiltonian of the electron.

In addition to the hydrogen bridge bond ECL employ two kinds of three-center bonds which they call the central and the linear three-center bonds. The former is the bond between three boron atoms, each at a corner of an equilateral triangle. Three atomic orbitals,  $\lambda_1$ ,  $\lambda_2$ , and  $\lambda_3$ ,

one on each atom pointing towards the center of the triangle combine to form one bonding and two degenerate antibonding orbitals, namely

$$v_1 = 3^{-\frac{1}{2}} (\lambda_1 + \lambda_2 + \lambda_3) \quad (b) \quad (1.4)$$

$$v_2 = 2^{-\frac{1}{2}} (\lambda_1 - \lambda_2) \quad (ab)$$

and 
$$v_3 = 6^{-\frac{1}{2}} (\lambda_1 + \lambda_2 - 2\lambda_3) \quad (ab)$$

The energy difference being  $3\beta$ . The linear three-center bond affords binding between three boron atoms lying on a straight line. The atomic orbital on the middle atom,  $\lambda_2$ , is assumed to be a p orbital with the nodal plane perpendicular to the line between the three atoms. The three atomic orbitals give rise to one bonding, one non-bonding (nb) and one antibonding orbital;

$$v_1 = 2^{-1} (\lambda_1 + 2^{+\frac{1}{2}}\lambda_2 - \lambda_3) \quad (b) \quad (1.5)$$

$$v_2 = 2^{-\frac{1}{2}} (\lambda_1 + \lambda_3) \quad (nb)$$

$$v_3 = 2^{-1} (\lambda_1 - 2^{+\frac{1}{2}}\lambda_2 - \lambda_3) \quad (ab)$$

The difference of energy between the bonding and the non-bonding orbital is  $2^{\frac{1}{2}}\beta$ .

ECL predict that in a boron hydride that contains all three kinds of bond the lowest electronic transition will, under the assumption that a transition is localized in one bond, be from the bonding to the non-bonding orbital of a linear three-center bond. It is easily seen that this transition is allowed for radiation with the electric vector along the line connecting the three atoms.

In decaborane ECL assumed the four equivalent hydrogen atoms to be bonded each to the two nearest boron atoms by a hydrogen bridge bond. The boron skeleton is held together by two two-center bonds (between atoms 2 and 6 and 4 and 9), four central three-center bonds (between atoms 1, 2, and 3; 1, 3, and 4; 1, 5, and 10; and 3, 7, and 8), and two linear three-center bonds (between atoms 5, 2, and 7 and 8, 4, and 10). The result is a closed shell structure where each boron atom is bonded to all its nearest neighbors. They predict the following order of electron density

$$(2,4) > (1,3) = (6,9) > (5,7,8,10)$$

and a dipole moment of 1.6 to 2.2 Debye.

According to ECL boron atom 2 is bonded to atoms 5 and 7 by a bond that can be described approximately as a linear three-center bond, the wavefunction of the bonding orbital being

$$v_1 = 2^{-1} (\lambda_5 + 2^{+\frac{1}{2}} \lambda_2 - \lambda_7) \quad (b) \quad (1.6)$$

where  $\lambda_5$  and  $\lambda_7$  are  $sp^3$  hybridized atomic orbitals on atoms 5 and 7 respectively, pointing towards atom 2, and  $\lambda_2$  is a p atomic orbital with the y-z molecular plane as nodal plane. The non-bonding orbital is

$$v_2 = 2^{-\frac{1}{2}} (\lambda_5 + \lambda_7) \quad (nb) \quad (1.7)$$

Boron atom 4 is bonded to atoms 8 and 10 in the same way:

$$v_3 = 2^{-1} (\lambda_8 + 2^{+\frac{1}{2}} \lambda_4 - \lambda_{10}) \quad (b) \quad (1.8)$$

$$v_4 = 2^{-\frac{1}{2}} (\lambda_8 + \lambda_{10}) \quad (nb)$$

being the bonding and non-bonding orbital respectively.

The lowest electronic transition in decaborane should then be  $v_2 \leftarrow v_1$  and  $v_4 \leftarrow v_3$ . But these four orbitals do not behave properly under the symmetry operations of the molecular point group  $C_{2v}$ . Proper functions are found by combination.

$$\phi(a_2) = 2^{-\frac{1}{2}} (v_1 + v_3) \quad (b) \quad (1.9)$$

$$\phi(b_1) = 2^{-\frac{1}{2}} (v_1 - v_3) \quad (b)$$

$$\phi(a_1) = 2^{-\frac{1}{2}} (v_2 + v_4) \quad (nb)$$

$$\phi(b_2) = 2^{-\frac{1}{2}} (v_2 - v_4) \quad (nb)$$

The index in parenthesis indicates the symmetry representation of the function (Table 4).

If there is no interaction between the three-center orbitals  $\phi(a_2)$  and  $\phi(b_1)$  and  $\phi(a_1)$  and  $\phi(b_2)$  form two sets of degenerate functions, but if the orbitals are allowed to interact one finds that

$$w(b_1) < w(a_2) \quad (1.10)$$

$$w(a_1) < w(b_2)$$

The selection rules under the point group allow two transitions,

$$\phi(b_2) \leftarrow \phi(a_2)$$

$$\phi(a_1) \leftarrow \phi(b_1)$$

both for light polarized along the molecular x-axis. One might, therefore, expect to find two absorption peaks in the ultraviolet.

A much more detailed calculation has recently been carried out by Moore, Lohr and Lipscomb (MLL)(32) using an LCAO molecular orbital analysis for the boron framework. They assume the ten external hydrogen atoms to be bonded by two-center bonds, and the remaining four hydrogen atoms to be bonded to the two nearest boron atoms by hydrogen bridge bonds, and thus solve the remaining 10-center 16-electron problem, delocalizing the orbitals completely. They too arrive at a closed shell structure, and the order of the electron density agrees with that expected from the chemical behaviour of decaborane:

$$(2,4) > (1,2) > (5,7,8,10) > (6,9)$$

The calculated dipole moment is 3.50 Debye in excellent agreement with the experimental value, 3.52 Debye.

The highest filled orbital according to MLL is  $\phi(b_1)$ ,  $w = -5.72$  ev, and there are two low-lying empty orbitals  $\phi(a_1)$ ,  $w = 6.43$  ev, and  $\phi(a_2)$ ,  $w = 6.77$  ev. It might be noted that this  $\phi(b_1)$  is essentially the same orbital as the  $\phi(b_1)$  that we constructed from the ECL three-center orbitals, but  $\phi(a_2)$  is localized mainly on boron atoms 5, 7, 8, and 10 and  $\phi(a_1)$  is completely delocalized.

The transitions

$$\phi(a_1) \longleftarrow \phi(b_1) \quad \Delta w = 12.15 \text{ ev}$$

$$\phi(a_2) \longleftarrow \phi(b_1) \quad \Delta w = 12.49 \text{ ev}$$

are both allowed, the former for radiation polarized along the molecular x-axis, the latter for radiation polarized along the y-axis, so again we might expect the absorption spectrum to consist of two peaks.

A simple approach was suggested by Pimentel and Pitzer (33), and used by them to interpret the absorption spectrum they observed. Decaborane is shaped roughly like half a sphere, and if the potential energy is smeared out, the Schrodinger equation becomes the equation for a free particle in a hemispherical box. This equation can be solved and the appropriate number of electrons placed in the energy levels obtained.

The angular part of the wavefunction is found to be the surface harmonics, and the selection rules are the same as for the hydrogen atom:

$$\Delta m = 0 \qquad z \text{ - polarized light}$$

and  $\Delta m = +1 \qquad x \text{ or } y \text{ polarized light.}$

The structure of decaborane was not accurately known at the time, so Pimentel and Pitzer assumed 24 electrons to be localized and were left with 20 "metallic" electrons. By adjusting the radius of the box so that the first allowed transition coincided with the observed absorption maximum at 2720 Å, they calculated the radius to be 3.60 Å.

Their calculations were repeated with two minor adjustments: It seems reasonable to include the bridgebonded hydrogens in the box, this increases the number of "metallic" electrons to 24. The distance between boron atoms 6 and 9 is 3.48 Å and the distance between atoms 5 and 8 is 3.31 Å (34). If the box is extended 0.5 Å beyond the boron framework, the radius is 2.2 Å. Under these assumptions it is found that the lowest allowed transition should be at 32000 cm<sup>-1</sup>, and is allowed for x or y polarized radiation. The next lowest transition is allowed for z polarized light and should occur at 97000 cm<sup>-1</sup>.



It appeared that a more thorough investigation of the absorption spectrum of decaborane, would be desirable, to answer some of the following questions: Is the transition reported by Pimentel and Pitzer electronically allowed? What is the symmetry of the excited state? Are there any other low-lying electronic states?

The answer to these questions would further provide a test for the accuracy of the theories outlined above.

## CHAPTER II

### EXPERIMENTAL

The decaborane was obtained from the Olin Matheson Corporation, and was purified by one sublimation at room temperature in a manner suggested by Dr. A. E. Newkirk (34). One or two grams of powdered decaborane were placed at the closed end of an 18 cm long, 35 mm diameter glass tube that terminated in a male standard-taper joint. This in turn was connected with a female standard-taper joint and a stopcock, and the system was evacuated to a pressure of ten microns before the stopcock was closed. The tube was then suspended in a horizontal position, and a small temperature gradient was established along it by hanging a piece of moist paper towel over the tube near the opening about 10 cm from the impure sample.

The decaborane sublimed over a period of several days to form clear, colorless crystals that were found to melt at 97.9-98.0° C (uncorrected). The reported melting point is 99.7° C (35). This material was used for gas-, solution-, and crystal-spectra without further purification. A small sample was sublimed twice more, but gave a crystal spectrum at liquid helium temperature that was identical with the spectra obtained with material sublimed only once.

2,4-Diiododecaborane was synthesized and purified as described by Hillman (36). The material used for absorption spectra melted at 256.5-257.0° C (uncorrected) while Hillman reports an (uncorrected) melting point of 261° C.

Solution Spectra.--The absorption spectra of decaborane and 2,4-diiodo-decaborane in solutions of cyclohexane and acetonitrile were measured with a Beckmann DK recording spectrophotometer. The first spectra were recorded using dried and redistilled chemicals off the shelf, but these were found to be of insufficient purity, as even small amounts of water would react with the solutes (37). Matheson, Coleman and Bell Spectrograde Solvents were therefore used for the final measurements.

The following solutions were prepared:

Solution I	1.69 mg $B_{10}H_{14}$ dissolved in 50 ml cyclohexane $C = 2.76 \times 10^{-4}$ mole/liter
Solution II	1.59 mg $B_{10}H_{14}$ dissolved in 50 ml cyclohexane $C = 2.60 \times 10^{-4}$ mole/liter
Solution III	105 mg $B_{10}H_{14}$ dissolved in 3 ml cyclohexane $C = 0.29$ mole/liter
Solution IV	1.56 mg $B_{10}H_{14}$ in 50 ml acetonitrile $C = 2.55 \times 10^{-4}$ mole/liter
Solution V	1.51 mg $B_{10}H_{14}$ in 50 ml acetonitrile $C = 2.47 \times 10^{-4}$ mole/liter
Solution VI	2.07 mg 2-4 $B_{10}H_{14}$ in 10 ml acetonitrile $C = 5.53 \times 10^{-4}$ mole/liter
Solution VII	2.02 mg 2-4 $B_{10}H_{12}I_2$ in 10 ml acetonitrile $C = 5.40 \times 10^{-4}$ mole/liter

As both decaborane and diiododecaborane react slowly with acetonitrile (38)(Appendix), the spectra were recorded immediately after the solutions had been prepared. The solubility of the diiododecaborane in cyclohexane was found to be so slight that no spectrum could be recorded in this solvent.

Gas Spectrum.---The absorption spectra of gaseous and crystalline decaborane were measured spectrographically. A 150 watt D.C. Hanovia Xenon Compact Arc Lamp 901 C-1 served as a source of intense ultraviolet radiation, and a 15 cm focal length quartz lens focused the radiation on the slit of the Jarrel-Ash JACO-Wadsworth Stigmatic three-meter Replica Grating Spectrograph. Two gratings were used, one with 15000, the other with 30000 lines per inch and both with a ruled area of length two inches and height one and a half inches. Exposures were made with slit widths varying from 20 to 100 microns which provides a resolution of approximately  $0.1 \text{ \AA}$  to  $0.5 \text{ \AA}$  with the 30000 lines per inch grating.

The spectrum of the mercury lamp from a Beckmann DU spectrophotometer was superposed on the absorption spectra and provided a basis for determination of wavelengths. Using the mercury lines at 3021.50, 3125.66, and  $3341.48 \text{ \AA}$  as standards, the wavelengths of 16 other atomic lines (A, Fe, Hg, W) were calculated by linear interpolation with a maximum error of  $0.15 \text{ \AA}$ , and an average error of  $0.08 \text{ \AA}$ . Since the lines in the absorption spectrum of crystalline decaborane proved to be broader than these atomic lines, they are believed to be determined with an accuracy of  $\pm 0.2 \text{ \AA}$ .

The spectra were photographed on Eastman Kodak 103-0 film which is sensitive from  $2400 \text{ \AA}$  to  $5000 \text{ \AA}$  (39). Due to the high intensity of

the source the exposure time never exceeded five minutes. The films were developed in Kodak Developer D 19, fixed in Kodak Rapid Liquid Fixer, and after they had been washed and dried, they were scanned on a Leeds and Northrup Recording Microphotometer.

The vapor pressure of decaborane at room temperature is less than 1 mm Hg (40) so it is necessary to heat the optical cell to obtain a sufficiently large optical path for the vapor-phase spectrum. A 43 cm long Pyrex cell with quartz windows was therefore wrapped in a sheet of asbestos paper and wound with number 30 B and S gage constantan wire which was covered with another sheet of asbestos. The temperature of the cell was measured with a copper-constantan thermocouple with one junction between the wall of the cell and the first layer of asbestos and the other in ice water.

Solid decaborane was introduced through a sidearm and the cell was evacuated, flushed with gaseous helium, re-evacuated to ten microns pressure and sealed off. It was found that 30 volts potential across the constantan wire which had a resistance of 70 ohms, was sufficient to raise the temperature of the cell to a hundred degrees centigrade and exposures were made at various temperatures ranging from 90°C to 130°C. These temperatures correspond to a pressure range of ten to fifteen mm Hg (41).

Crystal Spectra.--Preliminary studies were made employing crystals obtained by the sublimation technique described above. These crystals were needle shaped, two or three mm long and one mm thick, and they soon proved unsatisfactory in several ways: Their irregular shape led to tremendous loss of intensity by scattering, their thickness was so

great that the exposure times became large, and their diminutive size made the optical arrangement difficult. It was, therefore, necessary to find a way to grow thinner crystals with larger cross-sections.

This was done in the following way: Purified and powdered decaborane was placed between slides of fused quartz and melted under an infrared lamp. When cooled, the decaborane froze to form long, needle-like crystals. Some of the crystals were 5 mm long but were only a fraction of a mm broad. Fortunately the crystal axes of neighbouring crystallites proved to be nearly parallel, their orientation rarely differed by more than  $3^\circ$ , so large, approximately monocrystalline regions could be found and masked off. By using different spacers between the quartz slides and by applying pressure on them before the decaborane froze, the thickness which was determined by weight, could be varied from 6 to 250 microns.

The directions of the crystal axes were found under a polarizing microscope, and the axes were then identified by x-ray diffraction<sup>1</sup>. One of the two quartz slides covering the crystal was removed, and the other slide with the crystal was mounted in the Single Crystal Orienter of a General Electric X-Ray Diffraction Machine No. 5 (XRD-5) and rotated in search for strong reflections. With Cu  $K_\alpha$  radiation ( $\lambda = 1.54 \text{ \AA}$ ) the following reflections were found to be particularly strong:

$$\begin{array}{ll} \theta (400) = 12.3^\circ & \theta (040) = 8.5^\circ \\ \theta (002) = 15.7^\circ & \theta (004) = 32.8^\circ \end{array}$$

---

(1) The author would like to thank Dr. R. A. Young of the Georgia Tech Engineering Experiment Station for help with the x-ray work.

In the two crystals examined by x-ray techniques the direction of growth was along the b-axis (see Fig. 4). In both crystals the b-c plane was parallel to the surface of the slides while the a-axis was normal to them. It was therefore possible to measure the absorption of light polarized along the b and c axes, and in subsequent experiments crystals were oriented by their absorption spectrum.

A Wollaston prism was mounted directly behind the slit of the spectrograph in such a way that radiation with the electric vector in the horizontal plane (horizontally polarized radiation) was separated from radiation with the electric vector in the vertical plane (vertically polarized radiation). When the slit length was less than one mm, two separate, parallel spectra were recorded on the film. By placing a Glan prism of known orientation in front of the slit it was found that the top spectrum was due to horizontally polarized radiation while the lower spectrum was due to vertically polarized radiation.

The absorption of radiation polarized along the crystal b and c axes could thus be measured simultaneously by mounting the crystal in front of the spectrograph with one of the axes horizontal and the other vertical. It is, of course, vital for the comparison of the spectra obtained that the two beams of polarized radiation are equally intense. Due to the reflections inside the spectrograph this condition was not completely satisfied, and exposures were made with the crystal mounted with the b-axis both horizontal and vertical.

It was further found that our quartz lenses rotated the plane of polarization, and hence no focusing lens was used between the crystal and the slit.

The first low temperature measurements were made with the liquid nitrogen cell described by W. G. Trawick (42), but only one very weak, very broad band appeared in the spectrum. No attempt was made to measure the temperature of the crystal when mounted in the cell, but comparison with spectra obtained later when the crystal was immersed in liquid nitrogen showed that the temperature must have been considerably above 77°K.

For the studies at liquid helium temperature it was necessary to build a cryostat. Liquid helium boils at 4.2° K and the heat of vaporization is 0.75 cal/cc, as compared to 77.3° K and 38.6 cal/cc for liquid nitrogen (43), and hence care must be taken in the design of a liquid helium cryostat to minimize heat transfer through conduction or radiation. Several cryostats for optical studies have been described in the literature (44, 45), and the main features are usually the following: The helium container proper is suspended from a long neck and is insulated by a vacuum space followed by a liquid nitrogen-filled radiation shield which in turn is insulated from the outer wall of the cryostat by another vacuum space. All surfaces have been treated so they are highly reflective to minimize heat transfer by radiation.

The cryostats described in the literature are made of Pyrex-brand glass or metal. The construction of a cryostat from glass, however, requires a glassblowing lathe to handle the larger of the many concentric cylinders, and no such lathe was available to us at the time. To construct an all-metal system, a mass spectrograph is needed for leak testing of the vacuum jackets, and a mass spectrograph was also unavailable. We were, therefore, forced to design a simpler cryostat that could be



constructed with the means available. The cryostat that was built and used for measurements at liquid nitrogen and liquid helium temperatures is shown in Fig. 2.

The helium container or cryogenic container and the vacuum jacket were made of Pyrex Standard Wall tubing<sup>2</sup>. The cryogenic container had a capacity of 600 cc liquid, and terminated in a T-shaped quartz tube with optically flat, strain-free windows, manufactured to our specifications by Engelhard-Hanovia Industries. The Pyrex to quartz graded seal withstood the thermal shock of cooling to 4°K repeatedly without breaking. Connection to the vacuum jacket is made through a large, 75/102, ground ball joint, and the system is evacuated through a stopcock at the outer part of the neck.

The vacuum jacket is surrounded by a pair of loose-fitting, half-cylindrical buckets made of 1/16 inch copper sheet and held together by two large hose clamps. When the buckets were filled with liquid nitrogen, the vacuum jacket was cooled by conduction through the thin layer of air between the two parts. A three inches thick layer of Styrofoam served as thermal insulation of the copper buckets.

The sidearms of the vacuum jacket extended through the copper buckets and the Styrofoam and five cm into the room. This length was sufficient to keep the windows (strain-free, fused quartz slides cemented on by Apiezon Wax W) at room temperature, and no fogging occurred.

To prevent heat transfer by radiation, an attempt was made to silver the two glass parts. Both the Rochelle Salt Method (46) and

---

(2) The author would like to express his gratitude to Mr. Don E. Lillie who constructed these parts.

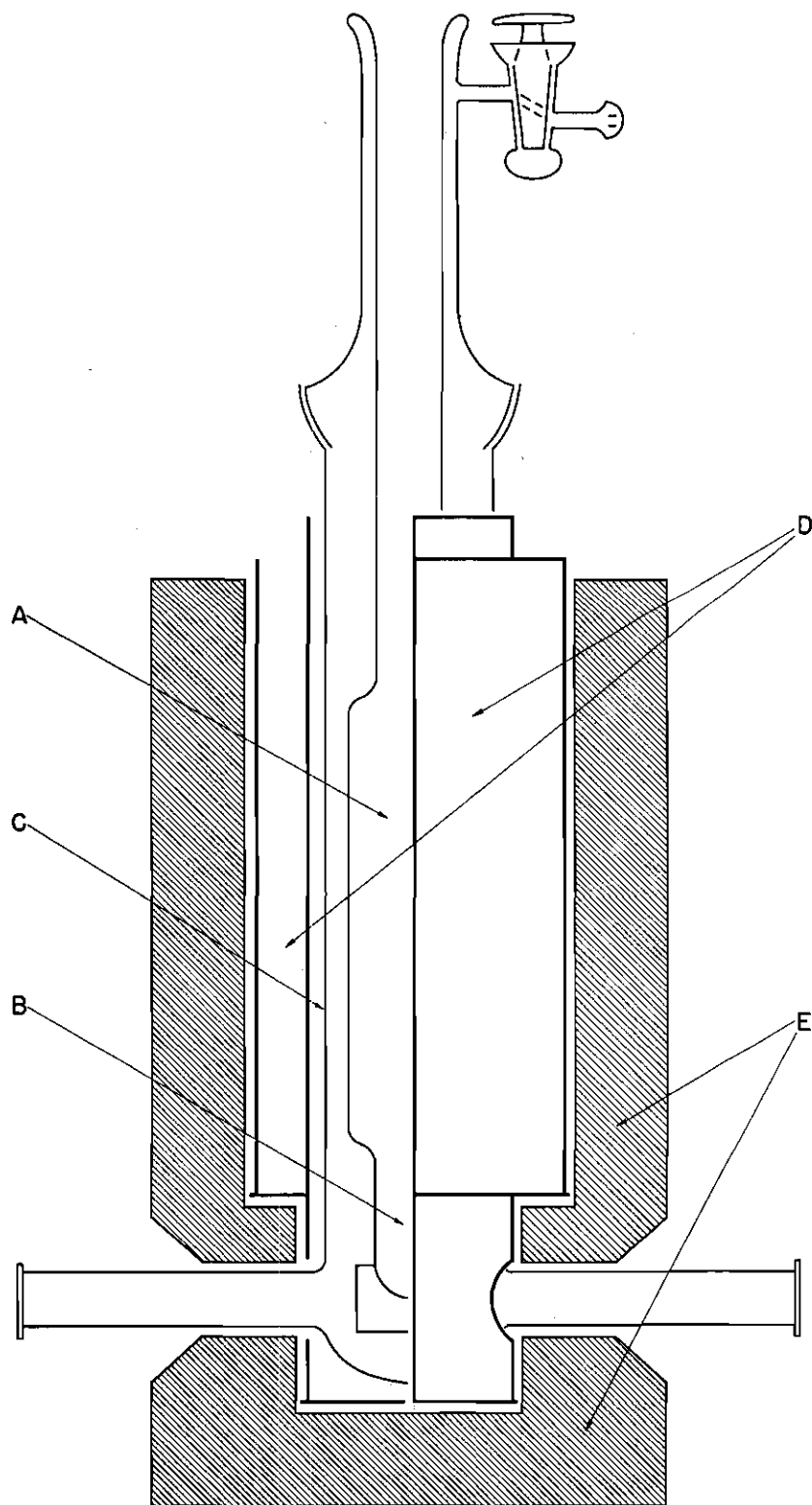


Figure 2. The Liquid Helium Cryostat. Cryogenic Container (A), T Shaped Quartz Tube (B), Vacuum Jacket (C), Copper Buckets (D), and Styrofoam Insulation (E).

the Brashear Method (47) were used, but proved unsatisfactory as the crucial surface, the face towards the vacuum space, invariably turned out dull. A shiny surface was obtained by painting on Hanovia Liquid Bright Gold No. 261, drying for a day, and firing to 560° C in an annealing oven. This method was both cheaper and easier than chemical silvering and gave a very shiny surface that proved both strong and durable.

The glass parts were suspended freely from the ball joint which was supported in a triangular hole in one-half inch plywood, and the copper buckets were held in place by the Styrofoam which was suspended in a Handy-Angle frame independently of the inner glass parts. This arrangement served to eliminate thermal and mechanical strain and also facilitated the optical alignment.

The pumping system was built for this experiment. A mechanical forepump was connected with an air-cooled oil diffusion pump (Consolidated Electrodynamics Corporation type VMF-21 pump) that according to the manufacturer should be capable of producing an ultimate pressure of  $1 \times 10^{-6}$  mm Hg. The rest of the system consisted of copper tubing, standard fittings, and high vacuum valves. All joints were silver-soldered with Easy Flo No. 45 solder and Handy Flux, and a thermocouple gauge for measuring pressures from 10 microns to 500 microns and a Philips ionization gauge sensitive over the region 0.01 micron to 1 micron Hg was connected. No leaks were found, and after continuous operation for the period of one month the pressure had decreased to 0.01 micron Hg as measured with the Philips gauge. When connected with the cryostat, the system produced a pressure of 0.02 micron Hg.

Liquid helium was obtained from the Linde Corporation in a 25 liter Supairco container, and was transferred to the cryostat through a transfer

tube of conventional design made from 0.035 inch wall Monel tubing<sup>3</sup>. It consisted of a 3/16 inch diameter inner tube and a 1/2 inch diameter outer tube. The vacuum space was evacuated through a 1/8 inch Hoke valve to a pressure of 0.1 micron before the valve was closed. Liquid helium could be pumped from the Supairco container to the cryostat by applying an excess pressure of two to three pounds per square inch gaseous helium above the liquid.

For studies at 77° K it was sufficient to fill the cryogenic container with liquid nitrogen without the copper buckets or Styrofoam insulation. One filling was found to last 24 hours.

For experiments at 4° K the copper buckets and the cryogenic container were first filled with liquid nitrogen for precooling. The liquid nitrogen was then forced out of the cryogenic container by gaseous helium and the liquid helium introduced. Both nitrogen and oxygen are solid at 4° K, and as small crystals of these substances make the helium turbid, great care must be taken to exclude air. The cryogenic container was swept out with gaseous helium before liquid helium was introduced, and air was prevented from diffusing in by introducing a rubber tube five cm down the neck and bleeding through it a slow stream of gaseous helium. The liquid nitrogen in the copper buckets was found to last two hours, while one filling of helium in the cryogenic container lasted one hour.

The stopcock connecting the vacuum space with the pumping line was closed prior to introduction of liquid helium. The vapor pressures of oxygen and nitrogen at 4.2° K are negligible, so these gases will

---

(3) The author is indebted to Dr. Edwin J. Schiebner for advice and assistance in the handling of liquid helium.

condense on the cryogenic container and the pressure will decrease below 0.02 micron Hg. The sample of crystalline decaborane was mounted at the end of an 85 cm long, thin-walled Monel tube, immersed in the cryogenic fluid, and suspended at the bottom of the T-shaped quartz tube with the slides parallel to the windows. Since liquid nitrogen evaporated from the surface only, spectra at  $77^{\circ}$  K could be obtained without further difficulty. But liquid helium boiled vigorously, and the bubbles led to loss of intensity by scattering and mixed the horizontally and vertically polarized radiation after it had passed through the crystal. However, by pumping on the liquid helium with a mechanical pump till it reached the lambda-point and then bleeding in gaseous helium to atmospheric pressure, the temperature of the liquid could be reduced below the boiling point, and several exposures could be made before the temperature again reached  $4.2^{\circ}$  K.

Once a crystal had been cooled below  $100^{\circ}$  K, it was found to crack when warmed to room temperature. The connection to the mechanical pump was therefore made in such a way that the crystal could be kept in the cryostat during the pumping: The opening of the cryogenic container was covered by a three inches high copper cap, resting on a 1/2 inch thick silicon rubber "washer" placed on top of the neck of the container. The Monel tube on which the decaborane was mounted, extended through a quick-coupler seal at the top of the cap and could thus be moved up and down at will. Connection to the mechanical pump and a cylinder of helium gas was made through the side of the cap. The atmospheric pressure on the cap was sufficient to give air tight connection during the pumping.

Glass Spectrum.--0.104 gm decaborane was dissolved in a mixture of 2.0 ml ethylether and 2.0 ml isopentane ( $c = 0.21$  mole/liter) and the solution introduced into a one cm long Pyrex optical cell. When the cell was immersed in liquid nitrogen in the cryostat, the solution solidified to a glass, and the spectrum was measured spectrographically. This glass could not be cooled to  $4.2^{\circ}$  K without crystallizing so no measurements on glasses were made at this temperature.

## CHAPTER III

### A REVIEW OF THE THEORY OF ELECTRONIC SPECTRA OF MOLECULAR CRYSTALS

The electronic absorption spectrum of a molecular crystal, such as decaborane, is so similar to that of the same compound in a gaseous or dissolved state, that it appears reasonable to attempt to describe the crystal in terms of the wavefunctions and energy levels of the free molecule. The interaction of the molecules in the crystal is then treated as a perturbation and must explain the differences between the spectra of the compound in a dilute and condensed system. The differences observed are the following:

- (1) The energy of the 0-0 transition may change.
- (2) Levels that are degenerate in the free molecule may be split in the crystal.
- (3) Transitions that are forbidden in the free molecule may appear with considerable intensity in the crystal.
- (4) Levels that are nondegenerate in the free molecule sometimes appear as doublets or triplets in the solid. (Davydov splitting).

During recent years the theory of absorption spectra of molecular crystals has received a great deal of attention (48, 49, 50, 51, 52). Here only the main features will be repeated, so that they can be referred to during the discussion of the absorption of radiation by monocrystalline decaborane in Chapter IV.

Let  $h$  be the Hamiltonian of a free molecule, and assume that  $\{\varphi^{(i)}\}$  is the set of all eigenfunctions such that

$$h \varphi^{(i)} = w^{(i)} \varphi^{(i)} \quad (3.1)$$

where  $w^{(i)}$  is the energy of the  $i$ 'th molecular state. Then each eigenfunction or set of degenerate eigenfunctions transforms like one of the irreducible representations of the point group that describes the molecular symmetry,  $M$ .

When a molecule is placed in a crystal, however, the Hamiltonian is no longer given by  $h$ , but

$$h' = h + V \quad (3.2)$$

where  $V$  is the interaction potential due to the other molecules in the crystal. Treating  $V$  as a perturbation we find that the new energy levels are given to the first order by:

$$w^{(i)'} = w^{(i)} + \int \varphi^{(i)} V \varphi^{(i)} d\tau \quad (3.3)$$

if the  $i$ 'th level is nondegenerate. If  $\varphi^{(i)}$  is a member of a degenerate set, the new energy levels are found by solving the secular equation:

$$\text{Det} \left[ \int \varphi^{(i)} h' \varphi^{(j)} d\tau - \delta_{ij} w \right] = 0 \quad (3.4)$$

for  $i$  and  $j$  running over the degenerate set. The energy of the transition

$\varphi^{(h)} \leftarrow \varphi^{(i)}$  is now given by

$$\Delta w^e = w^{(h)'} - w^{(i)'} \quad (3.5)$$

and the spectrum will shift accordingly.



The site in the crystal in which the molecule is located is characterized by a group of symmetry operations that leave the crystal invariant. This group, which is one of the 32 crystallographic point groups, is called the site group,  $S$ . We will denote the order of  $S$  by  $s$ . It is clear that  $V$  must have the full symmetry of  $S$ .  $S$  is a subgroup of  $M$ , which means that  $V$  need not have the full symmetry of the molecule, and even if  $\phi^{(i)}$  and  $\phi^{(j)}$  are degenerate

$$\int \phi^{(i)} V \phi^{(i)} d\tau \text{ need not be equal to } \int \phi^{(j)} V \phi^{(j)} d\tau$$

and a splitting of the level may result by solution of Equation (3.4).

Finally one often finds that functions that form a basis for different irreducible representations of  $M$  form a basis for the same representation of  $S$ . In that case the matrix element

$$(\phi^{(i)} | V | \phi^{(j)}) = \int \phi^{(i)} V \phi^{(j)} d\tau \quad (3.6)$$

need not be zero, and a mixing results:

$$\phi^{(i)'} = \frac{1}{N} \left( \phi^{(i)} - \sum_j \frac{(\phi^{(i)} | V | \phi^{(j)})}{w^{(j)} - w^{(i)}} \phi^{(j)} \right) \quad (3.7)$$

Now even if  $\phi^{(j)} \leftarrow \phi^{(i)}$  is forbidden,  $\phi^{(j)'} \leftarrow \phi^{(i)'}$  may become allowed if, for instance,  $\phi^{(k)} \leftarrow \phi^{(i)}$  is allowed and  $\phi^{(j)}$  has been mixed with  $\phi^{(k)}$  by the crystal field,  $V$ .

To put it in other words: The molecule in the crystal no longer has the full symmetry of the free molecule. The proper wavefunctions must transform properly under the site group only, and the selection rules are therefore determined by the symmetry of the site.

To explain the last phenomenon listed above, namely the apparent splitting in the crystal of levels that are non-degenerate in the free molecule, it is necessary to find the wavefunctions of the entire crystal. This can be done by combining the wavefunctions of the individual molecules in appropriate ways. An excited state of the crystal is described to a first approximation by assuming one molecule to be excited while all the others are in the ground state. Since we have already taken into account the interaction of different electronic levels of the molecule, we may now fix our attention on one excited level, and construct the wavefunction of the crystal which corresponds to having a molecule in this state.

In the following the prime will be omitted from the symbol of the perturbed molecular function, and the wavefunctions of the ground state denoted by  $\phi^0$  and the wavefunction of the excited state by  $\phi^i$  where the index i denotes the irreducible representation of the site group to which  $\phi^i$  belongs. It will be assumed that  $\phi^i$  is non-degenerate, and that the crystal contains only one set of equivalent molecules, that is, given the position of one molecule all others can be generated by applying the symmetry operations of the lattice. The first assumption is valid for decaborane as all levels are non-degenerate under the site group  $C_2$ , but the crystal proves to have two sets of equivalent molecules. However, the extension of the theory required to treat such a crystal is simple, and will be carried out later.

The Hamiltonian of the crystal is

$$H = \sum_{ab} h_{ab} + \sum_{ab>cd} V_{ab,cd} \quad (3.8)$$

where  $h_{ab}$  is the Hamiltonian of the molecule in site  $b$  in unit cell  $a$  in the absence of interaction, and  $V_{ab,cd}$  is the interaction potential between the molecule in site  $b$  in unit cell  $a$  and the molecule in site  $d$  in unit cell  $c$ . The terms are summed over all sites in all unit cells. In the following the crystal will be assumed to consist of  $N^3$  unit cells each with  $n$  molecules in the labeled sites.

The crystal is characterized by a set of symmetry elements that includes all primitive translations and also may include rotation axes, inversion centers, mirror planes, glide planes and screw axes. The corresponding symmetry operations form a group that is called the space group of the crystal,  $G$ . The order of  $G$  will be denoted by  $g$ . It is clear that the Hamiltonian has the full symmetry of the space group, and the wavefunctions of the crystal must therefore form a basis for the irreducible representations of  $G$ . In general the irreducible representations of  $G$  turn out to be of fairly high dimensions and the wavefunctions correspondingly complicated, but we shall show that the optically active levels are simple and indicate how their wavefunctions can be found.

The lowest energy level in the crystal arises when all the molecules are in their ground state. The wavefunction is given to the order of accuracy required here by the simple product:

$$\Psi^0 = \prod_a \prod_b \varphi_{ab}^0 \quad (3.9)$$

This function has the full symmetry of the crystal and therefore needs no further elaboration. But if we assume that one molecule is excited, we can write down  $n \times N^3$  degenerate functions:

$$\Phi_{kl}^i = \prod_a \prod_b \varphi_{ab}^i \quad (3.10)$$

where the product is taken over all molecules except molecule  $kl$ . None of these functions behaves properly under the space group, and they must therefore be combined in appropriate ways.

Since the group of all primitive translations,  $T$ , forms an invariant subgroup of the space group, (53) it is possible to express the latter as a sum of the form:

$$G = TR_1 + TR_2 + \dots + TR_r + \dots + TR_f \quad (3.11)$$

where  $R_1, R_2, \dots, R_f$  are elements in  $G$ , and  $R_1$  is the identity element,  $e$ . It can further be shown (54) that the cosets  $TR_r$  are the elements of a group with  $T$  as identity and that this group is isomorphic with one of the 32 crystallographic point groups. This group is called the factor group,  $F$ . The order of  $F$  is denoted by  $f$ , and since there are  $N^3$  primitive translations, Equation (3.11) shows that  $f \times N^3 = g$ . It should be noted that the elements in the factor group are uniquely determined even if the set of coefficients,  $\{R_r\}$ , is arbitrary to some extent.

This breakdown of  $G$  into cosets of  $T$  indicates that it might be convenient to begin our search for the irreducible representations of  $G$  by finding the irreducible representations of  $T$ . Each member,  $\underline{t}$ , of  $T$  can be expressed as

$$\underline{t} = m_1 \underline{t}_1 + m_2 \underline{t}_2 + m_3 \underline{t}_3 \quad (3.12)$$

where  $m_1, m_2$ , and  $m_3$  are integers and  $\underline{t}_1, \underline{t}_2$ , and  $\underline{t}_3$  are the primitive unit vectors. To make the group finite, cyclic boundary conditions are

adopted:

$$N\underline{t}_1 = N\underline{t}_2 = N\underline{t}_3 = e \quad (3.13)$$

Next we define a set of  $N^3$  vectors  $\underline{K}$  in the following way:

$$\underline{K} = \frac{1}{N} (p_1 \underline{b}_1 + p_2 \underline{b}_2 + p_3 \underline{b}_3) \quad (3.14)$$

where

$$p_1 = 0, 1, 2, \dots, N-1 \quad (3.15)$$

$$p_2 = 0, 1, 2, \dots, N-1$$

$$p_3 = 0, 1, 2, \dots, N-1$$

and the vectors  $\underline{b}_1$ ,  $\underline{b}_2$ , and  $\underline{b}_3$  are given by:

$$\underline{b}_1 \cdot \underline{t}_j = \delta_{ij} \cdot 2\pi \quad (3.16)$$

These three vectors define a unit cell in the reciprocal lattice and each  $\underline{K}$  is a vector from the origin to a point inside this unit cell.

For each  $\underline{K}$  it is easy to see that the set  $\{e^{i \underline{K} \cdot \underline{t}}\}$  is a representation of  $T$ . Since this representation is one-dimensional, it is irreducible and since there are  $N^3$  distinct vectors  $\underline{K}$ , we have found all the irreducible representations of  $T$ .

Let us select one representation of the translation group and see how it transforms under an element,  $R$ , of the space group. Since  $R$  is a member of a coset of the translation group (Equation (3.11))

$$R = \underline{t}_s R_r \quad (3.17)$$

for some  $r$  and  $s$ , and

$$\begin{aligned} \underline{t}_s R_r (e^{i \underline{K} \cdot \underline{t}}) &= \underline{t}_s (e^{i(R_r \underline{K}) \cdot (R_r \underline{t})}) \\ &= e^{i(R_r \underline{K}) \cdot (\underline{t}_s + R_r \underline{t})} \end{aligned} \quad (3.18)$$

In general  $R_r \underline{K}$  will be different from  $\underline{K}$ , under an inversion for instance

$$i \underline{K} = -\underline{K} \quad (3.19)$$

which is equivalent to

$$\underline{K}^+ = -\underline{K} + \underline{b}_1 + \underline{b}_2 + \underline{b}_3 \quad (3.20)$$

Since all the space group elements in the same coset of T differ only by a primitive translation, they will transform  $\underline{K}$  into the same vector. And unless  $\underline{K}$  lies in a symmetry element in the reciprocal lattice each coset will transform  $\underline{K}$  into a different vector. We define the set of vectors into which  $\underline{K}$  is transformed as the star of  $\underline{K}$ , denoted by  $\mathfrak{S}\underline{K}$ . For general  $\underline{K}$  the order of this set will be equal to  $f$ , the order of the factor group.

The irreducible representations of the space group can now be constructed from the irreducible representations of the translation group (55), but only the results will be indicated. A representation,  $e^{i \underline{K} \cdot \underline{t}}$ , of T will for general  $\underline{K}$  give rise to an irreducible representation of G of dimension  $f$ . The representatives of the primitive translations in G will be diagonal matrices of the form

$$(e^{i \underline{K}^+ \cdot \underline{t}})$$

where  $\underline{K}^+$  goes over all elements in  $\mathfrak{S}\underline{K}$ . But if  $\underline{K}$  lies on a symmetry element in the reciprocal lattice, the representations may be of smaller

dimensions, and if  $\underline{K} = \underline{0}$  the resulting representations of the space group are particularly simple.

By Equation (3.11)  $G$  was broken down into cosets of  $T$  that formed the elements of the factor group  $F$ , and we stated that  $F$  was isomorphic to one of the 32 crystallographic point groups. It is, therefore, relatively easy to find the irreducible representations of  $F$ , and from each irreducible representation of  $F$  we can construct one irreducible representation of  $G$ . Fixing our attention on one representation of  $F$  we assign to each space group element in a coset of  $T$  the representative of that coset considered as an element in  $F$ .

We now return to the problem of constructing the wavefunctions of the crystal by combining functions of the form

$$\Phi_{kl}^i = \varphi_{kl}^i \prod_a \prod_b \varphi_{ab}^0 \quad (3.21)$$

First we will form functions that transform properly under the group of primitive translations. The functions

$$\psi_1^i(\underline{K}) = N^{-3/2} \sum_k e^{i\underline{K} \cdot \underline{t}_k} \Phi_{kl}^i \quad (3.22)$$

where  $\underline{t}_k$  is the vector from the origin to unit cell  $k$ , are easily seen to form a basis for one of the irreducible representations of  $T$ , namely the representation  $\{e^{i\underline{K} \cdot \underline{t}}\}$ . And since there are  $N^3$  distinct values of  $\underline{K}$ , there are  $N^3$  such functions for each site  $l$ . The functions  $\psi_1^i(\underline{K})$  are called one-site excitons and represent a wave of excitation traveling over the sites  $l$  in all unit cells in the crystal. The vector  $\underline{K}$  is now called the wavevector. One-site excitons where the excitation travels

over other sites, can be written down in the same manner, and we thus obtain  $n \times N^3$  one-site excitons.

It is found that the symmetry operations of the space group transform the one-site excitons in a way that is similar to the way they transform the translation group representations: An operation transforms a one-site exciton  $\psi_1^i(\underline{K})$  into another  $\psi_b^i(\underline{K}^+)$  where  $\underline{K}^+$  is a member of  $\underline{S}\underline{K}$ .

The  $n \times f$  functions  $\psi_1^i(\underline{K}^+)$  for  $l$  running over all sites and  $\underline{K}^+$  running over all members of  $\underline{S}\underline{K}$ , must be combined to form bases for irreducible representations of the space group, and since, for general  $\underline{K}$ , these are of dimension  $f$ , the result must be  $n$  sets of  $f$ -fold degenerate functions. But group theory is of no further help in finding these functions, it is necessary to solve an  $nf \times nf$  secular equation.

For the one-site excitons with wavevector zero it is, however, possible to carry the treatment still further. These functions must be combined to form bases for the irreducible representations of the space group that are characterized by  $\underline{K} = 0$ , namely the representations constructed from the irreducible representations of the factor group. But this means that the new functions form a basis for the irreducible representations of the factor group. Since  $F$  is of much smaller order than  $G$ , it is more economical to carry out the discussion in terms of  $F$ , and we will therefore go on to find wavefunctions that will behave properly under  $F$ . These functions will then automatically transform properly under  $G$ .

The set of functions  $\psi_1^i(0)$  for running  $l$  form the basis for a reducible representation of  $F$ , and by reducing this representation in



the well known way, we will find the number of crystal wavefunctions,  $i n_j$ , that belong to the  $j$ 'th factor group representation. Except in cases of accidental degeneracy, functions belonging to different factor group representations will be of different energy and a splitting, called factor group splitting or Davydov splitting, will result. But before we try to find the reducible representation of  $F$ , it will be convenient to investigate the relations between the site group,  $S$ , and the factor group,  $F$ .

When the space group was broken down into cosets of the translation group:

$$G = TR_1 + TR_2 + \dots + TR_r + \dots + TR_f \quad (3.23)$$

it was stated that the cosets,  $\{TR_r\}$ , are uniquely determined while the set of coefficients,  $\{R_r\}$ , is arbitrary to some extent. Indeed, the cosets can be found by constructing the cosets  $TR$  for all  $R$  in  $G$ . This procedure will yield only  $f$  distinct cosets, namely the elements of the factor group. The set  $\{R_r\}$  may therefore be selected in any convenient way as long as the  $f$  cosets  $\{TR_r\}$  are distinct.

A site  $kl$  in the crystal is characterized by the site group  $S$ . The symmetry operations of  $S$  performed in the site  $kl$  are also members of the space group, and we will denote them by  $R_{S(kl)}$  and the group by  $S(kl)$ . The  $s$  cosets  $T R_{S(kl)}$  for all  $R_{S(kl)}$  in  $S(kl)$  are clearly distinct and can therefore be chosen to constitute the first  $s$  members of  $F$ . These cosets can easily be shown to form a subgroup of  $F$  that we shall denote by  $\{TR_{S(kl)}\}$ . A member of the site group,  $R_{S(kl)}$ , transforms a primitive translation into another primitive translation. Hence

any space group element  $tR_{S(kl)}$  in the coset  $TR_{S(kl)}$  will move a molecule in site 1 in unit cell a into the same kind of site, 1, in some unit cell c. The coset  $TR_{S(kl)}$  is therefore said to preserve the site 1.

Keeping in mind that the cosets in the factor group must be distinct, it is easy to show that the cosets  $TR_{S(kl)}$  are independent of our initial choice of unit cell k. Further it can be shown that a space group element  $tR$  that is contained in one of the f-s cosets that are not of the form  $TR_{S(kl)}$  must move a molecule in site 1 in unit cell a into some other kind of site, b, in some unit cell c. Hence the f-s last cosets in the factor group do not preserve site 1.

We will in the following assume that the cosets  $TR_{S(kl)}$  also preserve the other sites in the unit cell. This need not be so, but we shall see that the assumption is justified in the case of decaborane. The groups  $\{TR_{S(kl)}\}$  and  $\{TR_{S(kb)}\}$  are then identical, and by comparing the angular parts of the transformations we find that

$$TR_{S(kl)} = TR_{S(kb)} \quad (3.24)$$

if R is the same point group operation. From now on the indices (kl) will be omitted, and the collection of cosets that preserve sites will be denoted by  $\{TR_S\}$ .

Since  $\{TR_S\}$  is a subgroup of F, the latter can be expanded in cosets of the former:

$$F = \{TR_S\} + \{TR_S\} TR_{r1} + \dots + \{TR_S\} TR_{rq} \quad (3.25)$$

The factor group elements in each of these cosets must transform the site 1 in the same way. Since there are n sites for 1 to be transformed into,

there must be at least  $n$  cosets, but there cannot be more than  $n$  cosets as this would imply that some site is preserved by some factor group element not in  $\{TR_S\}$ . The order of  $F$  is thus  $n \times s = f$ .

We are now ready to find the character of the reducible representation of  $F$  for which the set of one-site excitons

$$\psi_1^i(\underline{0}) = N^{-\frac{3}{2}} \sum_k \varphi_{k1}^i \prod_a \prod_b \varphi_{ab}^0 \quad (3.26)$$

form a basis. If a coset  $TR_S$  preserves the site 1, the only effect on  $\psi_1^i(\underline{0})$  will be the transformation of the function  $\varphi_{k1}^i$  under the angular part  $R_S$ . Since  $\varphi_{k1}^i$  transforms like the  $i$ 'th irreducible representation of the site group we get the following contribution to the character of the representative of the coset:

$${}^i X_{1F}(TR_S) = X_S^i(R_S) \quad (3.27)$$

where  $X_S^i(R_S)$  is the character of  $R_S$  in the  $i$ 'th representation of  $S$ . If on the other hand the coset  $TR_R$  does not preserve the site 1, the contribution to the character must be zero. Hence

$${}^i X_{1F}(TR_R) = X_S^i(R_R) \delta_{S \cdot R_R} \quad (3.28)$$

where  $\delta_{S \cdot R_R}$  is one if  $R_R$  is contained in  $S$  and zero otherwise. Adding the contributions from all the one-site excitons we find the character of the representative of  $TR_R$ :

$${}^i X_F(TR_R) = \sum_1^i X_{1F}(TR_R) \quad (3.29)$$

$$\begin{aligned}
 &= \sum_l X_S^i(R_r) \delta_{S \cdot R_r} \\
 &= n X_S^i(R_r) \delta_{S \cdot R_r} \quad 4
 \end{aligned}$$

Using the orthogonality of the irreducible representation of F, we can reduce the representation above. The number of times,  ${}^i n_j$ , that the j'th irreducible representation of F occurs is given by

$${}^i n_j = \frac{1}{f} \sum_{TR_r \text{ in } F} {}^i X_F(TR_r) X_F^i(TR_r) \quad (3.30)$$

$$= \frac{1}{f} \sum_{TR_r \text{ in } F} n X_S^i(R_r) \delta_{S \cdot R_r} X_F^j(TR_r)$$

$$= \frac{1}{f} \sum_{TR_r \text{ in } \{TR_S\}} n X_S^i(R_r) X_F^j(TR_r)$$

$${}^i n_j = \frac{n}{f} \sum_{R_S \text{ in } S} X_S^i(R_S) X_F^j(TR_S) \quad (3.31)$$

S is isomorphic to the subgroup  $\{TR_S\}$  of F. That means that the representatives of  $\{TR_S\}$  in the j'th irreducible representation of F must also form a representation of S. The number of times the i'th irreducible representation of S is contained in this representation is given by

$$a_{ij} = \frac{1}{s} \sum_{R_S \text{ in } S} X_F^j(TR_S) X_S^i(R_S) \quad (3.32)$$

---

(4) The last step is justified by our assumption that the same cosets preserve all sites.

Substituting this into Equation (3.31) above, we get

$$i_{n_j} = \frac{n}{f} s a_{ij}$$

or 
$$\underline{i_{n_j} = a_{ij}} \quad (3.33)$$

since  $n \times s = f$ .  $a_{ij}$  can be found from the character tables of the site and factor group. Knowing the symmetry properties of the wavefunctions, the proper combinations of the one-site excitons,  $\psi_1^i(\underline{0})$ , can be written down by inspection.

We have now indicated how the  $n \times N^3$  degenerate functions  $\Phi_{kl}^i$  can be combined to form wavefunctions,  $\Psi^i(\underline{K})$ , of the entire crystal. These functions are no longer degenerate, but form a broad band. It might therefore be expected that a crystal spectrum would lack fine structure, and this is indeed the case at higher temperatures, but when the crystal is cooled below  $100^\circ\text{K}$  sharp lines appear, and the lines become sharper as the temperature is decreased. This behaviour is due to a stringent selection rule on  $\underline{K}$ . The transition moment between two states can be broken down into integrals involving two one-site excitons:

$$\begin{aligned} & \int \Psi_1^i(\underline{K}) \mp \Psi_1^h(\underline{K}') d\tau \quad (3.34) \\ &= \bar{N}^3 \sum_{\underline{k}} e^{i(\underline{K}-\underline{K}') \cdot \underline{t}_k} \int \Phi_{hl}^i \mp \Phi_{hl}^h d\tau \\ &= \bar{N}^3 \sum_{\underline{k}} p e^{i(\underline{K}-\underline{K}') \cdot \underline{t}_k} \end{aligned}$$

where  $p$  is the transition moment of one molecule

$$P = \int \Phi^i \underline{r} \Phi^h d\tau \quad (3.35)$$

By summing over  $k$  we find that the transition moment between the one-site excitons is identically zero unless

$$\underline{K} - \underline{K}' = 0$$

or, 
$$\underline{\Delta K} = 0 \quad (3.36)$$

At low temperatures each molecule is in its lowest, nonvibrating state, and the wavefunction is totally symmetric:

$$\Psi^0(\underline{0}) = \prod_k \prod_l \Phi_{kl}^0 \quad (3.37)$$

Transitions from this state are only allowed to excited states with wavevector zero. It is a fortunate circumstance that these are the very functions that we have shown can be written down from symmetry considerations alone. But not all of these states are optically active; since the ground state is totally symmetric, the transition moment

$$\int \Psi^0(\underline{0}) \underline{r} \Psi^i(\underline{0}) d\tau \quad (3.38)$$

is only different from zero if  $\Psi^i(\underline{0})$  transforms like one of the primitive unit vectors  $\underline{t}_1$ ,  $\underline{t}_2$ , or  $\underline{t}_3$ . Hence only a very limited number of transitions can appear at low temperatures.

The energy of the ground state of the crystal,  $W^0$ , is found from the wavefunction (Equation (3.9)) and the crystal Hamiltonian (Equation (3.8))

$$W^0 = \int \Psi^0 H \Psi^0 d\tau = (\Psi^0 | H | \Psi^0) \quad (3.39)$$

$$W^0 = \left( \prod_a \prod_b \varphi_{ab}^0 \mid \sum_{ab} h_{ab} \mid \prod_a \prod_b \varphi_{ab}^0 \right)$$

$$+ \left( \prod_a \prod_b \varphi_{ab}^0 \mid \sum_{ab>cd} V_{ab,cd} \mid \prod_a \prod_b \varphi_{ab}^0 \right)$$

$$W^0 = n N^3 w^0 + \frac{1}{2} n N^3 \sum_{ab \neq kl} (\varphi_{ab}^0 \varphi_{kl}^0 \mid V_{ab,kl} \mid \varphi_{ab}^0 \varphi_{kl}^0)$$

where the sum of interactions extends over all molecules in the crystal except  $kl$ . In most cases  $w^0$  is little affected by the perturbation under the site group, so  $n N^3 w^0$  is the energy of  $n N^3$  free molecules in their ground state. The term

$$-D = -\frac{1}{2} n N^3 \sum_{ab \neq kl} (\varphi_{ab}^0 \varphi_{kl}^0 \mid V_{ab,kl} \mid \varphi_{ab}^0 \varphi_{kl}^0) \quad (3.40)$$

is then the heat of sublimation of the crystal.

Since the wavefunctions of the optically active excited states were formed from linear combination of one-site excitons with wave-vector zero, the energy will be determined primarily by matrix elements of the form

$$W_1^i = (\psi_1^i(\underline{0}) \mid H \mid \psi_1^i(\underline{0})) \quad (3.41)$$

Moreover, since all sites in the crystal are equivalent  $W_1^i$  must be the same for all  $l$ . Substituting Equation (3.26), and remembering that  $\varphi_{kl}^i$  and  $\varphi_{kl}^0$  are orthogonal, one obtains:

$$\begin{aligned}
W_1^i &= (n N^3 - 1) w^0 + w^i & (3.42) \\
&+ \frac{1}{2} \sum_{ab \neq kl} (\varphi_{kl}^i \varphi_{ab}^0 | V_{ab,kl} | \varphi_{kl}^i \varphi_{ab}^0) \\
&+ \frac{1}{2} \sum_{cd \neq kl} \sum_{\substack{ab \neq cd \\ ab \neq kl}} (\varphi_{ab}^0 \varphi_{cd}^0 | V_{ab,cd} | \varphi_{ab}^0 \varphi_{cd}^0) \\
&+ \frac{1}{2} \sum_{a \neq k} (\varphi_{al}^i \varphi_{kl}^0 | V_{al,kl} | \varphi_{al}^0 \varphi_{kl}^i)
\end{aligned}$$

where  $kl$  is held constant in each sum. Since the energies of all one-site excitons are equal, the energies of the various factor group states will differ by cross terms of the form:

$$C = (\psi_1^i, (0) | H | \psi_1^i (0)) \quad (3.43)$$

which can be reduced to

$$C = \frac{1}{2} \sum_a (\varphi_{al}^i, \varphi_{kl}^0 | V_{al,kl} | \varphi_{al}^0, \varphi_{kl}^i) \quad (3.44)$$

To calculate the amount of splitting it is necessary to find an explicit form for  $V_{ab,cd}$ . The favored approach is to approximate  $V_{ab,cd}$  by a point multipole-multipole interaction, and disregard all except the first non-vanishing terms. If the dipole-dipole interaction term is different from zero;

$$V_{ab,cd} = -\frac{e^2}{3R_{ab,cd}^3} \sum (2 q_{1ab} q_{1cd} - q_{2ab} q_{2cd} - q_{3ab} q_{3cd}) \quad (3.45)$$

where  $e$  is the charge of the electron,  $R$  the inter-molecular distance, and  $q_{1ab}$ ,  $q_{2ab}$ , and  $q_{3ab}$  and  $q_{1cd}$ ,  $q_{2cd}$ , and  $q_{3cd}$  are the coordinates of an electron on molecule  $ab$  and  $cd$  respectively. The sum is extended



over all electrons in each molecule. The molecular axes are defined so that the two  $q_1$ -axes coincide, and the  $q_2$ - and  $q_3$ -axes form parallel pairs. This expression gives:

$$C = -\frac{1}{2} \sum_a \frac{e^2}{R_{al^i,kl}^3} (\Phi_{al^i}^o, \Phi_{kl^i}^i \mid \sum 2 q_{1ab} q_{1cd} - q_{2ab} q_{2cd} - q_{3ab} q_{3cd} \mid \Phi_{al^i}^i, \Phi_{kl^i}^o) \quad (3.46)$$

$$C = -\frac{1}{2} \sum_a \frac{p^2}{R_{al^i,kl}^3} (2 \cos \theta_{1al^i} \cos \theta_{1kl^i} - \cos \theta_{2al^i} \cos \theta_{2kl^i} - \cos \theta_{3al^i} \cos \theta_{3kl^i})$$

where  $p$  is the transition moment.

$$p = (\Phi^i \mid \underline{r} \mid \Phi^o) \quad (3.47)$$

and the angles  $\theta$  are the angles between the transition moment and the molecular axes,  $q$ .

The magnitude of the transition moment may be calculated or estimated from the absorption of the substance in solution:

$$p^2 (\text{cm}^2) = 3.97 \cdot 10^{-20} \int \epsilon \frac{d\nu}{\nu} \quad (3.48)$$

where  $\epsilon$  is the molar extinction coefficient and the integral extends over the entire band.

However, this procedure is correct only in the case of very strong interaction, when the coupling is much greater than the vibrational increments. As the amount of interaction decreases it becomes necessary to count the interaction between individual vibronic levels.

and as the interaction decreases further and becomes much less than the vibrational increments it is sufficient to calculate interactions between vibronic levels of the same energy. In this case  $p$  is the transition moment of a single vibronic transition, and the integration in Equation (3.48) is carried over only the corresponding vibronic peak. Denoting the halfwidth of the entire electronic band by  $\Delta$ , Peterson and Simpson (56) find the following criteria for weak, intermediate and strong coupling

$$\begin{array}{lll}
 2 C \ll \Delta & \text{weak coupling} & (3.49) \\
 2 C = \Delta & \text{intermediate coupling} & \\
 2 C \gg \Delta & \text{strong coupling} &
 \end{array}$$

In the next chapter the theory as outlined will be used to discuss the absorption spectrum of crystalline decaborane. We shall see that decaborane crystal contains two sets of equivalent sites, but that the theory can be applied without modification to each set separately. The site group will be found to be  $C_2$ , while the factor group will be found to be isomorphic to  $C_{2h}$ . Using the character tables of these groups and Equation (3.33) we shall show that an  $A_1$  or  $A_2$  excited state of the free molecule will give rise to four excited states of the crystal characterized by wavevector zero; one  $A_g$  and one  $A_u$  state for each set of equivalent sites. A  $B_1$  or  $B_2$  excited state of the free molecule will give rise to four excited crystal states with wavevector zero; one  $B_g$  and one  $B_u$  state for each set of equivalent sites.

Transitions from a totally symmetric ground state to  $A_g$  or  $B_g$  excited states are forbidden, while transitions to  $A_u$  and  $B_u$  states are allowed for radiation polarized along different crystal axes. On

the bases of absorption of polarized radiation by monocrystalline decaborane we shall be able to conclude that the excited crystal state is a  $B_u$  state, and hence that the excited state of the free molecule is of  $B_1$  or  $B_2$  symmetry.

Finally we shall allow the two  $B_u$  states to interact and calculate the resulting splitting with the help of Equation (3.46). Decaborane will prove to exhibit only weak intermolecular coupling, and the splitting will be found to be too small to be observed.

## CHAPTER IV

### RESULTS AND DISCUSSION

Solution Spectra.--The main features of the solution spectra are summarized in Table 2.

The absorption spectrum of decaborane in cyclohexane was recorded from 3600 Å to 2300 Å at 25° C and was found to exhibit one simple peak without any indication of shoulders and with maximum absorption at  $2700 \pm 10$  Å. The absorption appeared to begin at  $3200 \pm 50$  Å, or  $31250 \pm 500$  cm<sup>-1</sup>. This was in so marked disagreement with Pimentel and Pitzer (57) who reported the absorption to begin at  $3600 \pm 50$  Å, that Solution III which is nearly twice as concentrated as the most concentrated solution used by these workers, was prepared. This solution exhibited no absorption above 3370 Å; at 3300 Å the molar extinction coefficient is less than 0.5, and at 3250 Å it is 1.6 and is increasing rapidly.

In view of the fact that the sample employed in this investigation had a sharper melting point than theirs (97.9 - 98.0° C as compared to 99.3° - 99.6° C) it appears likely that the long wavelength absorption observed by Pimentel and Pitzer is due to impurities. The 0-0 transition in cyclohexane can then be localized at  $3250 \pm 50$  Å or  $30750 \pm 500$  cm<sup>-1</sup>.

The magnitude of the transition moment was determined by graphical integration over the band (Equation 3.48):



$$\underline{p^2 = 0.21 \times 10^{-16} \text{ cm}^2}$$

and the oscillator strength of the transition was found from

$$f = 4.33 \times 10^{-9} \int \epsilon(\omega) d\omega$$

Graphical integration gave

$$\underline{f = 0.10}$$

Table 2. Absorption Spectra of Solutions of  $B_{10}H_{14}$  and 2,4- $B_{10}H_{12}I_2$  at  $25^\circ \text{ C}$ .

	Solution No.	Wavelength of Maximum Absorption	Maximum Molar Extinction Coefficient ( $\text{Mol}^{-1}\text{cm}^{-1}$ )
I.	$B_{10}H_{14}$ in $C_6H_6$	$2700 \pm 10 \text{ \AA}$ ( $2720 \pm 50 \text{ \AA}$ ) <sup>5</sup>	2950 ( $3200 \pm 100$ ) <sup>5</sup>
II.	"-	"-	2710
IV.	$B_{10}H_{14}$ in $CH_3CN$	$2630 \pm 10 \text{ \AA}$	2820
V.	"-	"-	2750
VI.	2,4- $B_{10}H_{12}I_2$ in $CH_3CN$	$3130 \pm 10 \text{ \AA}$	1590
VII.	"-	"-	1480

The band halfwidth was found to be

$$\underline{\Delta = 7000 \text{ cm}^{-1}}$$

(5) Values reported by Pimentel and Pitzer (57).

The absorption spectrum of decaborane in acetonitrile also consists of one simple peak, but the absorption begins at  $3100 \pm 50 \text{ \AA}$  and the maximum is shifted to  $2630 \pm 10 \text{ \AA}$ .

The energy of the 0-0 transition is hence  $1000 \text{ cm}^{-1}$  less in the nonpolar solvent, cyclohexane, than in the polar solvent, acetonitrile. Since the electronic transition is in the boron framework, the interaction between solvent and solute can be assumed to be a dipole-dipole interaction, where the solvent molecules are placed around the solute molecule in the energetically favored way, and the energy of each electronic state is lowered by an amount that increases with the dipole moment of the state. It then follows from the observed blueshift in acetonitrile that the excited state of decaborane has a smaller dipole moment than the ground state.

Spectra of 2,4-diododecaborane in acetonitrile at  $25^\circ \text{ C}$  were recorded from  $5600 \text{ \AA}$  to  $2300 \text{ \AA}$ . In addition to a peak at  $3130 \pm 10 \text{ \AA}$  there is clear indication of a much stronger peak below  $2300 \text{ \AA}$ .

Gas Spectrum.--The absorption of gaseous decaborane was measured with optical paths ranging from 0.57 to 0.85 cm atm at temperatures from  $90$  to  $140^\circ \text{ C}$ , and was found to begin at  $3215 \pm 20 \text{ \AA}$  in excellent agreement with the assignment of the 0-0 transition in cyclohexane solution. The absorption increases rapidly towards shorter wavelengths, but no vibrational structure was found. It is known that decaborane is decomposed by ultraviolet radiation (58), hence this lack of structure might be due to dissociation.

Glass Spectrum.--The absorption spectrum of decaborane in solid solution in isopentane-ether at  $77^\circ \text{ K}$  was found to begin at  $3100 \text{ \AA}$  and increase

rapidly towards shorter wavelength, but the spectrum showed no structure.

Crystal Spectra.--The absorption of radiation polarized along the b and c crystal axes was measured at room temperature, at liquid nitrogen temperature, and at liquid helium temperature. Different crystals studied ranged in thickness from 6 to 250 microns.

At room temperature the absorption of radiation polarized along the b-axis seems to begin at  $3225 \pm 10 \text{ \AA}$ . No structure is found, but when the crystal is cooled to  $77^\circ \text{ K}$  some diffuse lines appear, and at  $4^\circ \text{ K}$  the spectrum exhibits several sharp lines. The first line is observed at  $3219.0 \text{ \AA}$ , no absorption is found on the long wavelength side of this line even with the thickest crystals. As the wavelength decreases the lines become broader, and it becomes increasingly difficult to distinguish them from the continuous background. Thus, although the wavelength of the first line is believed to be determined with an accuracy of  $\pm 0.2 \text{ \AA}$ , the uncertainty has increased to  $\pm 2 \text{ \AA}$  at  $3019 \text{ \AA}$ , and beyond this point the spectrum appears to be continuous. All lines found are listed in Table 3, and microphotometer traces of the spectrum are presented in Fig. 3.

At room temperature radiation polarized along the crystal c-axis is transmitted down to  $3100 \text{ \AA}$ , and as the temperature of the crystal decreases the transmittancy increases. Even at  $4.2^\circ \text{ K}$  the radiation suffers loss of intensity on passing through the crystal, but no structure is observed, and hence this loss is believed to be due to scattering. It is therefore concluded that the transition moment has a component along the crystal b-axis, but none along the c-axis.

Table 3. Absorption Lines of Radiation Polarized Along the b-Axis of Monocrystalline Decaborane at 4.2° K.

WAVELENGTH (Å)	WAVENUMBER (cm <sup>-1</sup> )	DESCRIPTION	VIBRATIONAL ASSIGNMENT		
			V <sub>1</sub>	V <sub>2</sub>	V <sub>3</sub>
3219.0	31057	st sh	0	0	0
3212.3	122	st vb		-	
3189.7	342	w		-	
3181.8	420	w		-	
3179.0	448	st sh	0	1	0
3175.5	482	st sh	1	0	0
3173.3	504	w		-	
3170.0	537	w		-	
3168.8	549	w		-	
3165.4	582	m sh	0	1	1
3161.9	617	m sh	1	0	1
3160.1	636	w		-	
3153.4	702	shoulder		-	
3152.1	715	st sh	0	1	2
3146.6	771	shoulder		-	
3144.2	795	st b		-	
3140.7	831	st sh	0	2	0
3137.5	863	st sh	1	1	0
3133.4	905	st sh	2	0	0
3129.4	946	w		-	
3126.9	971	m b		-	
3125.2	988	m b		-	
3123.2	32010	shoulder		-	
3121.9	023	w		-	
3117.6	066	st b		-	
3114.8	096	st b		-	
3111.5	130	shoulder		-	
3103.4	213	st b	0	3	0
3100.9	240	st b	1	2	0
3096	290	st b	2	1	0
3094	310	shoulder	3	0	0
3092	330	shoulder		-	
3086	390	w b		-	
3082	440	w b		-	
3076	470	w b		-	
3073	530	w b		-	
3070	560	w b		-	
3064	620	w b	1	3	0
3062	650	w b	2	2	0
3059	680	w b		-	
3055	720	w b	4	0	0
3025	33050	w b	3	2	0
3019	110	w b	5	0	0

w = weak  
vb = very broad

m = medium  
b = broad

st = strong  
sh = sharp



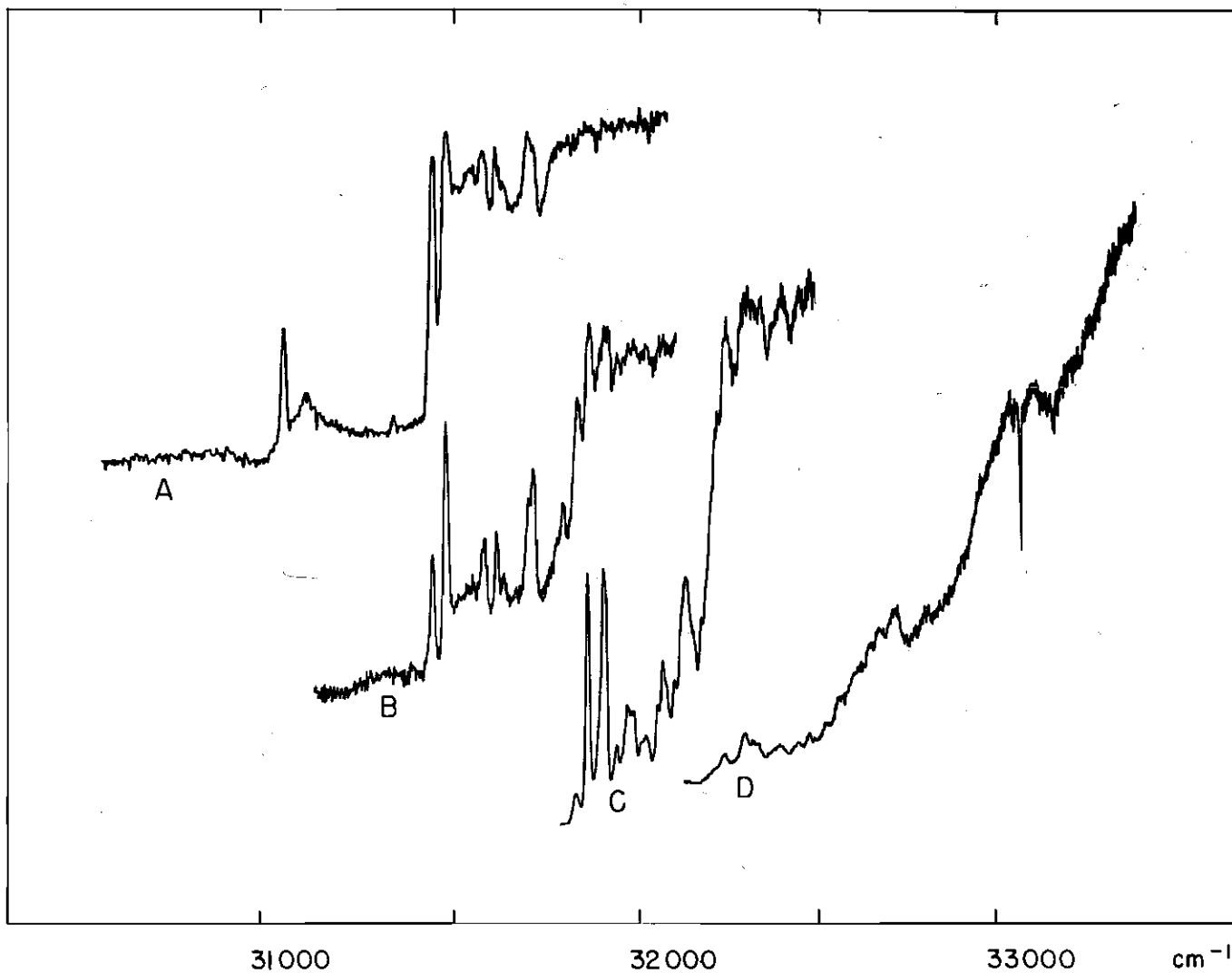


Figure 3. Absorption of Radiation Polarized along the b-Axis of Monocrystalline Decaborane at 4.2°K. Crystal Thickness: 200 microns (A), 15 microns (B and C), and 6 microns (D).

In order to interpret the spectrum it is necessary to consider the crystal structure. Kasper, Lucht and Harker (59) found the crystal to be monoclinic, but pseudoorthorhombic of class  $C_{2h}^4$  (60). The unit cell used by these workers is shown in Fig. 4A. It contains eight molecules lying in a plane (the a-b plane) with the molecular z-axis parallel to the crystal c-axis, but with the positive part of the z-axis pointing up or down as shown. The unit cell dimensions are:  $\underline{a} = 14.45 \text{ \AA}$ ,  $\underline{b} = 20.88 \text{ \AA}$ , and  $\underline{c} = 5.68 \text{ \AA}$ .

The crystal is highly twinned in the b-direction; the unit cell of the twin lattice can be formed from the unit cell in Fig. 4A by a  $180^\circ$  rotation around the b-axis followed by the non-primitive translation

$$\underline{t} = \frac{1}{4} (\underline{a} + \underline{b})$$

We will, however, consider decaborane as an ideal crystal, and return to discuss effects arising from the twinning later.

A primitive unit cell is shown in Fig. 4B. It contains four molecules in sites labeled  $\alpha$ ,  $\beta$ ,  $\gamma$ , and  $\delta$ . Each site contains a two-fold rotation axis normal to the plane of the paper, and the site group,  $S$ , is thus  $C_2$  for all sites. In addition to the two-fold rotation axes the space group includes inversion centers, glide planes and combinations of these with the primitive translations (61). The primitive vectors corresponding to this unit cell are  $\underline{t}_1 = \underline{a}$ ,  $\underline{t}_2 = \frac{1}{2}(\underline{a} + \underline{b})$ , and  $\underline{t}_3 = \underline{c}$ .

Denoting the set of all primitive translations by  $T$  and the set of space group elements by  $G$ ,  $G$  can be broken down into cosets of  $T$ :

$$G = Te + Tc_2 + T\sigma_h + Ti \quad (4.1)$$

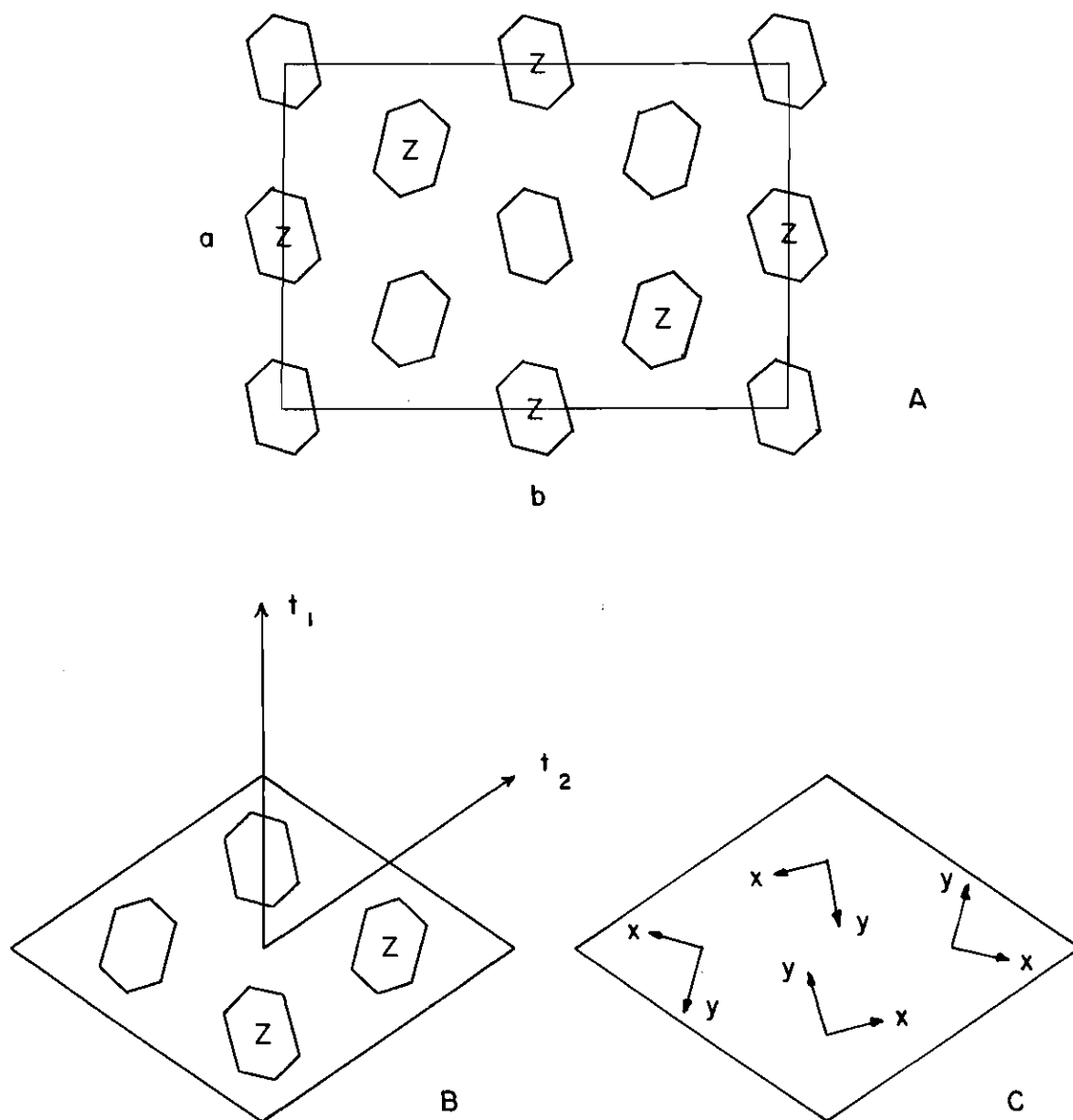


Figure 4. Crystal Structure of Decaborane. Unit Cell According to KLH (A), Primitive Unit Cell (B), and the Directions of the Molecular Axis (C). (Molecules marked Z have the positive part of the molecular z-axis above the plane of the paper).

where  $e$ ,  $c_2$ ,  $\sigma_h$ , and  $i$  are the identity operation, a two-fold rotation, a glideplane, and an inversion operation respectively. The factor group,  $F$ , is therefore of order four, and by writing down the multiplication table it is found to be isomorphic with the point group  $C_{2h}$ . The character tables of the molecular point group,  $M$ , and the site and factor group are collected in Table 4.

The elements of the factor group are found to exchange sites in the following way:

$Te$	no exchange
$Tc_2$	no exchange
$T\sigma_h$	$\alpha$ exchanged with $\gamma$ $\beta$ exchanged with $\delta$

Table 4. The Character Tables of the Molecular Pointgroup, the Site Group, and the Factor Group of Decaborane.

$C_{2v} = M$		$e$	$c_2$	$\sigma_x$	$\sigma_y$	
	$A_1$	1	1	1	1	$z$
	$A_2$	1	1	-1	-1	
	$B_1$	1	-1	-1	1	$x$
	$B_2$	1	-1	1	-1	$y$
$C_2 = S$		$e$	$c_2$			
	$A$	1	1	$z$		
	$B$	1	-1	$x,y$		
$F$		$Te$	$Tc_2$	$T\sigma_h$	$Ti$	
	$A_g$	1	1	1	1	
	$A_u$	1	1	-1	-1	$t_3$
	$B_g$	1	-1	-1	1	
	$B_u$	1	-1	1	-1	$t_1, t_2$

Ti                     $\alpha$    exchanged with  $\gamma$   
                           $\beta$    exchanged with  $\delta$

Decaborane thus contains two sets of equivalent sites,  $\{\alpha, \gamma\}$  and  $\{\beta, \delta\}$ , and all sites are preserved by the same cosets,  $T_e$  and  $T_{c_2}$ .

In chapter III it was assumed that the crystal contained only one set of equivalent sites, so the results obtained there cannot be applied to decaborane without comment.

The first effect of the crystalline state is to perturb the wavefunctions of the free molecule,  $\{\Phi^{(i)}\}$ , to give a new set of molecular functions that transform like one of the irreducible representations of the site group. If all sites were equivalent, the new functions and the corresponding energies would be identical for all molecules in the crystal, but it is not obvious that this is true for non-equivalent sites. Again considering the interaction potential,  $V$ , as a perturbation, the energy of a molecule in the ground state is given by first order perturbation theory:

$$w_{k\alpha}^{(o)'} = w^{(o)} + \sum_{ab \neq k\alpha} \left( \Phi_{k\alpha}^{(o)} \Phi_{ab}^{(o)} \left| V_{k\alpha, ab} \right| \Phi_{k\alpha}^{(o)} \Phi_{ab}^{(o)} \right) \quad (4.2)$$

$$w_{k\beta}^{(o)'} = w^{(o)} + \sum_{ab \neq k\beta} \left( \Phi_{k\beta}^{(o)} \Phi_{ab}^{(o)} \left| V_{k\beta, ab} \right| \Phi_{k\beta}^{(o)} \Phi_{ab}^{(o)} \right)$$

where  $w^{(o)}$ ,  $w_{k\alpha}^{(o)'}$ , and  $w_{k\beta}^{(o)'}$  are the energies of a free molecule, a molecule in site  $k\alpha$ , and a molecule in site  $k\beta$  respectively.

The two energies are found to be equal: For each  $\alpha$ - $\alpha$  interaction in  $w_{k\alpha}^{(o)'}$  there is a corresponding  $\beta$ - $\beta$  interaction in  $w_{k\beta}^{(o)'}$ , and for each  $\alpha$ - $\gamma$  interaction in the former there is a corresponding  $\beta$ - $\delta$  interaction in the latter. (This may not be apparent from the unit cell Fig. 4B, but

$V_{k\alpha, k\gamma} = V_{k\beta, k'\delta}$  where  $k' = k + t_2$ ). Furthermore, for each  $\alpha - \delta$  interaction in the former there is a  $\beta - \gamma$  interaction in the latter (found by an inversion operation), and the same  $\alpha - \beta$  interaction terms are found in both sums.

The energies of the  $i$ 'th excited state are given by:

$$w_{k\alpha}^{(i)'} = w^{(i)} + \sum_{ab \neq k\alpha} (\varphi_{k\alpha}^{(i)} \varphi_{ab}^{(o)} | V_{k\alpha, ab} | \varphi_{k\alpha}^{(i)} \varphi_{ab}^{(o)}) \quad (4.3)$$

$$w_{k\beta}^{(i)'} = w^{(i)} + \sum_{ab \neq k\beta} (\varphi_{k\beta}^{(i)} \varphi_{ab}^{(o)} | V_{k\beta, ab} | \varphi_{k\beta}^{(i)} \varphi_{ab}^{(o)})$$

Again the  $\alpha - \alpha$  interactions match the  $\beta - \beta$  interactions and  $\alpha - \gamma$  interactions match  $\beta - \delta$  interactions. And if  $V$  is approximated by a point multipole-multipole interaction, and if terms higher than quadrupole-quadrupole interaction are disregarded, the  $\alpha - \beta$  and  $\alpha - \delta$  interactions in  $w_{k\alpha}^{(i)'}$  are found to be equal to the  $\beta - \alpha$  and  $\beta - \gamma$  interactions in  $w_{k\beta}^{(i)'}$ . We, therefore, conclude that the energies of molecular states are identical for all molecules in the crystal.

The wavefunctions are found from second order perturbation theory. The mixing of wavefunctions of the free molecule is determined by matrix elements of the form:

$$(\varphi_{k\alpha}^{(h)} | V | \varphi_{k\alpha}^{(i)}) = \sum_{ab \neq k\alpha} (\varphi_{k\alpha}^{(h)} \varphi_{ab}^{(o)} | V_{k\alpha, ab} | \varphi_{k\alpha}^{(i)} \varphi_{ab}^{(o)}) \quad (4.4)$$

and

$$(\varphi_{k\beta}^{(h)} | V | \varphi_{k\beta}^{(i)}) = \sum_{ab \neq k\beta} (\varphi_{k\beta}^{(h)} \varphi_{ab}^{(o)} | V_{k\beta, ab} | \varphi_{k\beta}^{(i)} \varphi_{ab}^{(o)})$$

Under the approximation of  $V$  mentioned in the previous paragraph, the matrix elements are found to be equal, and we conclude that the wavefunctions also are identical for all molecules in the crystal.

Denoting the wavefunction of the ground state of a molecule in the crystal by  $\varphi^0$  and the wavefunction of an excited state by  $\varphi^i$ , we can now construct the  $4N^3$  degenerate functions

$$\bar{\Phi}_{kl} = \varphi_{kl}^i \prod_a \prod_b \varphi_{ab}^0 \quad (4.5)$$

as in Chapter III. Fixing our attention on the  $2N^3$  functions where the exciton is in the same set of equivalent sites, e.g.,  $\{a, \gamma\}$ , the arguments in Chapter III can be repeated step by step. The  $\bar{\Phi}$ -functions are combined to form one-site excitons, and the one-site excitons with wavevector zero must in turn be combined to form bases for the irreducible representations of the factor group, the number of crystal wavefunctions belonging to each factor group representation given by Equation (3.32) and Equation (3.33). Since the selection rule  $\Delta K = 0$  still is valid, these will be the only optically active states at low temperatures.

In decaborane the distinction between an  $A_1$  and  $A_2$  state of the free molecule is removed by the perturbation calculations; both give rise to an  $A$  site group state. The number of crystal wavefunctions belonging to the  $A_g$  factor group representation arising from one-site excitons  $\psi_a^A(\underline{0})$  and  $\psi_\gamma^A(\underline{0})$  is:

$$\begin{aligned} n_{A_g}^{A_{A,A_g}} &= \frac{1}{2} [X_S^A(e) X_F^{Ag}(Te) + X_S^A(c_2) X_F^{Ag}(Tc_2)] \\ &= \frac{1}{2} (1 \times 1 + 1 \times 1) = 1 \end{aligned} \quad (4.6)$$

Further we find

$$n_{A_u}^{A_{A_u}} = 1 \quad (4.7)$$

$$A_{n_{B_g}} = a_{A, B_g} = \frac{1}{2} [X_S^A(e) X_F^{B_g}(Te) + X_S^A(c_2) X_F^{B_g}(Tc_2)] \quad (4.8)$$

$$= \frac{1}{2} [1 \times 1 + 1 \times (-1)] = 0$$

$$A_{n_{B_u}} = 0 \quad (4.9)$$

Similarly it is found that a  $B_1$  or  $B_2$  state of the free molecule gives rise to one  $B_g$  and one  $B_u$  state of the crystal. From the character table of  $F$ , Table 4, we see that transitions from a totally symmetric,  $A_g$ , ground state is allowed to an  $A_u$  excited state for radiation polarized along the crystal  $c$ -axis and to a  $B_u$  excited state for radiation polarized along the crystal  $a$ - or  $b$ -axis, while transitions to  $A_g$  and  $B_g$  states are forbidden.

In the same manner it is found that an  $A_1$  or  $A_2$  state of the free molecule will give rise to the two one-site excitons  $\psi_\beta^A(\underline{0})$  and  $\psi_\delta^A(\underline{0})$  on the other set of equivalent sites, which in turn will combine to one  $A_g$  and one  $A_u$  crystal state, and a molecular  $B_1$  or  $B_2$  excited state of the free molecule will yield the one-site excitons  $\psi_\beta^B(\underline{0})$  and  $\psi_\delta^B(\underline{0})$  which will combine to one  $B_g$  and one  $B_u$  crystal state. Hence whatever the symmetry of the excited state of the free molecule, the crystal will have two optically active excited states, either two  $A_u$  states or two  $B_u$  states. These results are summarized in Table 5.

Since the crystal absorbs radiation polarized along the  $b$ -axis, while radiation polarized along the  $c$ -axis is transmitted, the excited crystal states must be  $B_u$  states, which means that the excited molecular state is either a  $B_1$  or a  $B_2$  state. The molecular state could be a vibronic coupling (62) of an  $A_2$  electronic state with a  $b_1$  or  $b_2$  vibra-



tion, but this appears unlikely as an  $A_2$  electronic state would mix with  $A_1$  states under the crystal field perturbation, the transition would

---

Table 5. Relations Between Molecular and Crystal States of Decaborane.

EXCITED MOLECULAR STATE	SITE STATE	CRYSTAL STATE	TRANSITION MOMENT
$A_1, A_2$	A	$A_g (\alpha, \gamma)$	o
		$A_u (\alpha, \gamma)$	c-axis
		$A_g (\beta, \delta)$	o
		$A_u (\beta, \delta)$	c-axis
$B_1, B_2$	B	$B_g (\alpha, \gamma)$	o
		$B_u (\alpha, \gamma)$	a- and b-axis
		$B_g (\beta, \delta)$	o
		$B_u (\beta, \delta)$	a- and b-axis

$(\alpha, \gamma)$ : exciton traveling over sites  $\alpha$  and  $\gamma$ .

$(\beta, \delta)$ : exciton traveling over sites  $\beta$  and  $\delta$ .

---

borrow intensity from the  $A_1$  transitions, and we should observe absorption of radiation polarized along the crystal c-axis. Such borrowing of intensity is observed in crystalline benzene where the 4.71 eV transition to a  $B_{2u}$  state becomes allowed through perturbation by other states, mainly an  $E_{1u}$  state at 6.76 eV (63).

It is therefore concluded that the symmetry of the free excited molecule is either  $B_1$  or  $B_2$  and that the transition is allowed.

Since no absorption is observed on the long wavelength side of the line at  $3219.0 \text{ \AA}$  this line must correspond to the 0-0 transition to the

lowest of the  $B_u$ -states if they are non-degenerate or to both if they are degenerate...

The wavefunctions of the two optically active excited states are:

$$\Psi_{\alpha, \gamma}^{B_u} = 2^{-\frac{1}{2}} [\psi_{\alpha}^{B(0)} - \psi_{\gamma}^{B(0)}] \quad (4.10)$$

$$\Psi_{\beta, \delta}^{B_u} = 2^{-\frac{1}{2}} [\psi_{\beta}^{B(0)} - \psi_{\delta}^{B(0)}]$$

Using the Hamiltonian of the crystal (Equation (3.8)) the energy of the first state is found to be

$$\begin{aligned} W_{\alpha, \gamma}^{B_u} &= (\Psi_{\alpha, \gamma}^{B_u} | H | \Psi_{\alpha, \gamma}^{B_u}) \quad (4.11) \\ &= \frac{1}{2} (\psi_{\alpha}^{B(0)} | H | \psi_{\alpha}^{B(0)}) \\ &\quad + \frac{1}{2} (\psi_{\gamma}^{B(0)} | H | \psi_{\gamma}^{B(0)}) \\ &\quad - (\psi_{\alpha}^{B(0)} | H | \psi_{\gamma}^{B(0)}) \end{aligned}$$

Which, by Equation (3.42) and Equation (3.44) reduces to:

$$\begin{aligned} W_{\alpha, \gamma}^{B_u} &= (4N^3 - 1) w^0 + w^B \\ &\quad + \frac{1}{4} \sum_{ab \neq ka} (\varphi_{ka}^B \varphi_{ab}^0 | V_{ab, ka} | \varphi_{ka}^B \varphi_{ab}^0) \\ &\quad + \frac{1}{4} \sum_{cd \neq ka} \sum_{\substack{ab \neq cd \\ ab \neq ka}} (\varphi_{ab}^0 \varphi_{cd}^0 | V_{ab, cd} | \varphi_{ab}^0 \varphi_{cd}^0) \\ &\quad + \frac{1}{4} \sum_{a \neq k} (\varphi_{aa}^B \varphi_{ka}^0 | V_{aa, ka} | \varphi_{aa}^0 \varphi_{ka}^B) \end{aligned}$$

$$\begin{aligned}
& + \frac{1}{4} \sum_{ab \neq k\gamma} (\varphi_{k\gamma}^B \varphi_{ab}^0 \mid V_{ab,k\gamma} \mid \varphi_{k\gamma}^B \varphi_{ab}^0) \\
& + \frac{1}{4} \sum_{cd \neq k\gamma} \sum_{\substack{ab \neq cd \\ ab \neq k\gamma}} (\varphi_{ab}^0 \varphi_{cd}^0 \mid V_{ab,cd} \mid \varphi_{ab}^0 \varphi_{cd}^0) \\
& + \frac{1}{4} \sum_{a \neq k} (\varphi_{a\gamma}^B \varphi_{k\gamma}^0 \mid V_{a\gamma,k\gamma} \mid \varphi_{a\gamma}^0 \varphi_{k\gamma}^B) \\
& - \frac{1}{4} \sum_a (\varphi_{aa}^B \varphi_{k\gamma}^0 \mid V_{aa,k\gamma} \mid \varphi_{aa}^0 \varphi_{k\gamma}^B)
\end{aligned}$$

The energy of  $\Psi_{\beta,\delta}^{B_u}$  is found by systematically exchanging  $\alpha$  with  $\beta$  and  $\gamma$  with  $\delta$  in the expression above, and the two energies are found to be equal just as when we considered excitation localized on one molecule (Equation (4-3)). The functions  $\Psi_{\alpha,\gamma}^{B_u}$  and  $\Psi_{\beta,\delta}^{B_u}$  therefore, appear to be degenerate.

However, the matrix element of the crystal Hamiltonian between the two functions is found to be different from zero:

$$\begin{aligned}
C &= (\Psi_{\alpha,\gamma}^{B_u} \mid H \mid \Psi_{\beta,\delta}^{B_u}) \quad (4.13) \\
&= \frac{1}{2} (\psi_{\alpha}^B(\underline{0}) \mid H \mid \psi_{\beta}^B(\underline{0})) - \frac{1}{2} (\psi_{\alpha}^B(\underline{0}) \mid H \mid \psi_{\delta}^B(\underline{0})) \\
&\quad - \frac{1}{2} (\psi_{\gamma}^B(\underline{0}) \mid H \mid \psi_{\beta}^B(\underline{0})) + \frac{1}{2} (\psi_{\gamma}^B(\underline{0}) \mid H \mid \psi_{\delta}^B(\underline{0}))
\end{aligned}$$

Which by symmetry reduces to

$$\begin{aligned}
C &= (\psi_{\alpha}^B(\underline{0}) \mid H \mid \psi_{\beta}^B(\underline{0})) - (\psi_{\alpha}^B(\underline{0}) \mid H \mid \psi_{\delta}^B(\underline{0})) \quad (4.14) \\
C &= (\psi_{\alpha}^B(\underline{0}) \mid V \mid \psi_{\beta}^B(\underline{0})) - (\psi_{\alpha}^B(\underline{0}) \mid V \mid \psi_{\delta}^B(\underline{0}))
\end{aligned}$$

The matrix element of  $V$  between the one-site excitons can be calculated by means of Equation (3.46) if the magnitude and orientation of

the transition moment,  $p$ , is known. The magnitude of  $p$  was determined from the absorption spectrum of decaborane in cyclohexane:

$$p^2 = 0.21 \cdot 10^{-16} \text{ cm}^2$$

but the orientation is unknown. The matrix elements were therefore calculated under two assumptions:

- (1)  $p$  is directed along the molecular x-axis
- (2)  $p$  is directed along the molecular y-axis

Under the first assumption

$$2 C (B_1) = -380 \text{ cm}^{-1}$$

when interaction with the 72 nearest neighbours is taken into account, while the second assumption gave

$$2 C (B_2) = 200 \text{ cm}^{-1}$$

It should be noted that the question of convergence of the series in Equation (3.46) should be considered. In the case of decaborane, however, there are interactions of different signs that lead to nearly perfect cancellation when  $R$  is greater than  $10 \text{ \AA}$ .

Since the width of the entire electronic band,  $\Delta$ , was found to be  $7000 \text{ cm}^{-1}$ ,

$$2 C \ll \Delta$$

in either case, and we have a case of weak coupling in the nomenclature of Peterson and Simpson (see Equation 3.49<sup>11</sup>). Thus, only vibronic states of the same energy interact.

Since the matrix element of the crystal Hamiltonian between the wavefunctions  $\Psi_{\alpha,\gamma}^{B_u}$  and  $\Psi_{\beta,\delta}^{B_u}$  is different from zero, better wavefunctions of the crystal are found by solving a  $2 \times 2$  secular equation. This gives

$$\Psi_+^{B_u} = 2^{-\frac{1}{2}} (\Psi_{\alpha,\gamma}^{B_u} + \Psi_{\beta,\delta}^{B_u}) \quad (4.15)$$

$$\Psi_-^{B_u} = 2^{-\frac{1}{2}} (\Psi_{\alpha,\gamma}^{B_u} - \Psi_{\beta,\delta}^{B_u})$$

the difference in energy being

$$2 C' = 2 (\Psi_{\alpha,\gamma}^{B_u} | H | \Psi_{\beta,\delta}^{B_u}) \quad (4.16)$$

when the matrix element is between equal vibronic levels only.

To calculate the splitting of the 0-0 line it is necessary to know the magnitude and direction of the transition moment of the 0-0 transition. Assuming the line at 3219.0 Å to correspond to one of the 0-0 transitions, the order of magnitude of  $p$  can be estimated: A 70 micron thick crystal was found to have about 10 per cent transmission at this wavelength, corresponding to a molar extinction coefficient of 18. The halfwidth is 19  $\text{cm}^{-1}$  and the integral

$$\int \epsilon \frac{d\nu}{\nu} = 18 \times \frac{19}{31000}$$

and the transition moment is found from Equation (3.48).

$$p^2 = 4.4 \times 10^{-22} \text{ cm}^2$$

Assuming  $p$  to be directed along the molecular x-axis and counting interaction with 72 nearest neighbours one finds

$$2 C' (B_1) = -8 \times 10^{-3} \text{ cm}^{-1}$$

or, if  $p$  is directed along the molecular y-axis

$$2 C' (B_2) = 4 \times 10^{-3} \text{ cm}^{-1}$$

Transitions from the totally symmetric ground state  $\Psi^0$  to the two excited states  $\Psi_{+}^{B_u}$  and  $\Psi_{-}^{B_u}$  should hence give two lines, spaced less than  $0.01 \text{ cm}^{-1}$  apart. However, in the current experiment the resolution is about  $5 \text{ cm}^{-1}$  so the two lines will appear as one, namely the line at  $3219.0 \text{ \AA}$ .

As the wavelength decreases the absorption lines become more intense. The transition moment and hence the splitting increases accordingly, which might account for the increasing broadness of the absorption lines below  $3130 \text{ \AA}$ . It appears then that the structure which is observed must be entirely due to vibrations, and since the electronic transition is allowed, the vibrations are probably totally symmetric.

It is seen from Fig. 5 that 18 of the 42 lines observed (and these 18 include all strong, sharp lines) can be explained by three vibrational increments:

$$\begin{aligned} \nu_1 &= 425 \text{ cm}^{-1} \\ \nu_2 &= 390 \text{ cm}^{-1} \\ \nu_3 &= 135 \text{ cm}^{-1} \end{aligned}$$

Even if these frequencies correspond to vibrations of the excited state of decaborane, they are so low that they may be assigned to boron-framework vibrations.

Conspicuous among the lines that do not fit into this vibrational scheme is the very broad, very strong line at  $3212 \text{ \AA}$  (see Fig. 3). The integrated intensity appears to be considerable, and the halfwidth is five times the halfwidth of the 0-0 lines at  $3219.0 \text{ \AA}$ . It seemed reasonable to assume that the broadness is due to some lattice defect

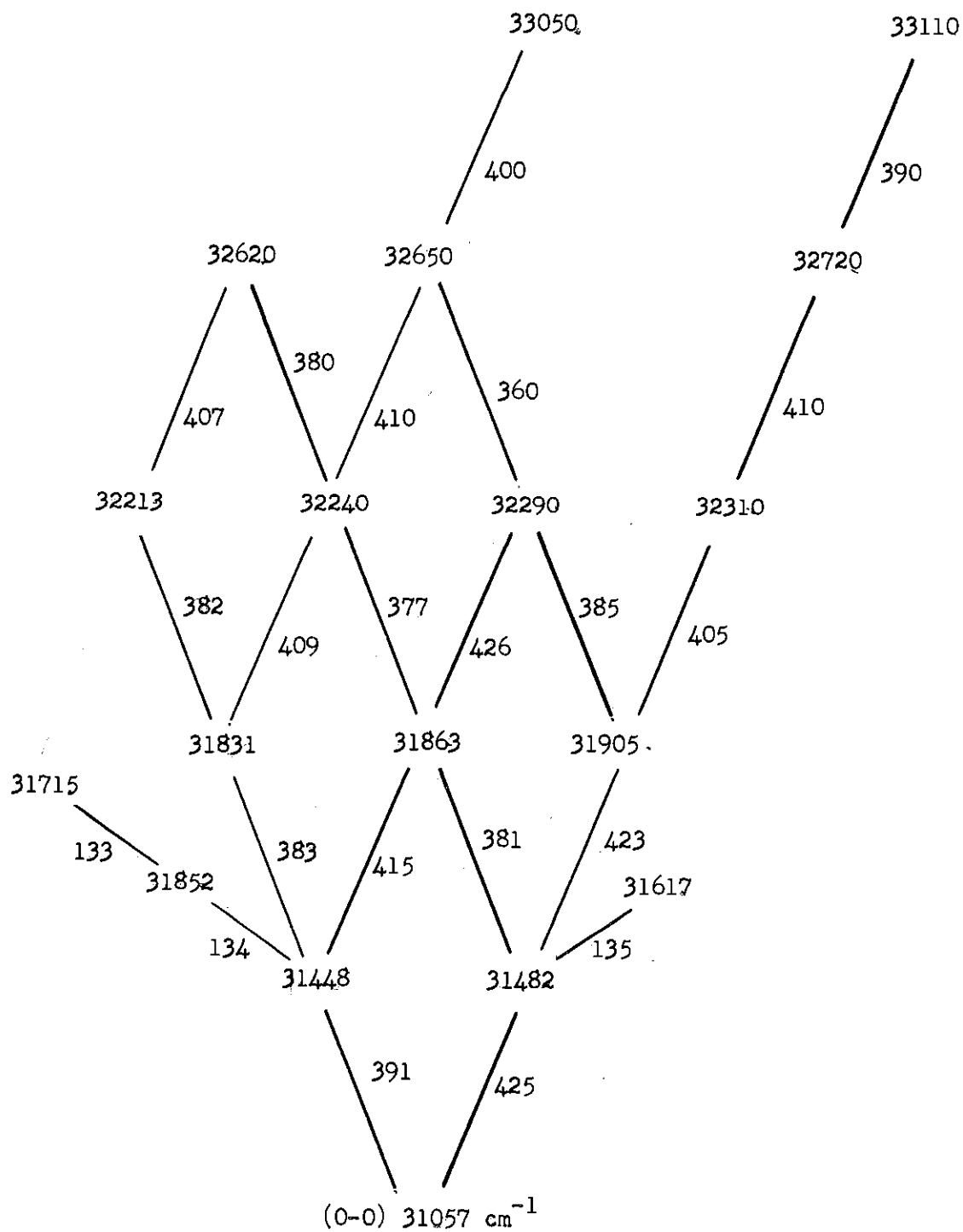


Figure 5. Vibrational Structure of the Spectrum of Crystalline Decaborane

that would lead to a break-down in the selection rule on  $\underline{K}$  and a corresponding broadening of the line.

It was mentioned briefly above that the x-ray studies showed decaborane to be highly twinned in the b-direction (64). Denoting the twin with unit cell as shown in Fig. 4A by Twin A, the unit cell of twin B can be obtained from the unit cell of Twin A by a rotation of  $180^\circ$  around the b-axis followed by the non-primitive translation  $1/4 (\underline{a} + \underline{b})$ . Kasper, Lucht and Harker found that the probability for a unit cell of Twin A to be followed by a unit cell B was 1:20. An idealized model of the twinned decaborane crystal can therefore be constructed in the following way: An asymmetric unit is formed from two crystal sheets, infinite in the a and c direction but only  $20 \underline{b}$  thick. One of the sheets is of type A and the other of type B, and this asymmetric unit is then repeated every  $40 \underline{b}$ .

The wavefunctions of the optically active states of the crystal can then be constructed from the wavefunctions of the optically active states of each sheet, and the corresponding energy levels calculated. The lack of periodicity in the real crystal (or the varying sheet thickness) would tend to make these levels diffuse. The spectral lines will be broad, but the maxima are not expected to shift.

Given the wavefunctions of the two sheets in the asymmetric unit the wavefunctions of the idealized twinned crystal can be found in a manner completely analogous to the method employed in finding the wavefunctions of an untwinned crystal from the wavefunctions of the molecule: We have a new primitive vector  $= 40 \underline{b}$  and form one-sheet (A or B) excitons characterized by a wavevector  $\underline{L}$ . The optically active excited states would again have  $\underline{L} = 0$ .



If the wavefunctions of each sheet can be assumed to have cyclic boundary conditions, the wavefunctions of the optically active excited states of the sheets are given by

$$\Psi_+^{B_u} \text{ (Twin A),} \quad \Psi_-^{B_u} \text{ (Twin A)} \quad (4.17)$$

and

$$\Psi_+^{B_u} \text{ (Twin B),} \quad \Psi_-^{B_u} \text{ (Twin B)}$$

while the ground state wavefunctions are

$$\Psi^{\circ} \text{ (Twin A)} \quad \text{and} \quad \Psi^{\circ} \text{ (Twin B)} \quad (4.18)$$

Combining these functions we find that the energies of the resulting wavefunctions with  $\underline{L} = 0$  differ only by matrix elements of the form

$$(\Psi^{\circ} \text{ (Twin A)} \Psi_b^B(\underline{0}) \text{ (Twin B)} \mid v \mid \Psi^{\circ} \text{ (Twin B)} \psi_d^B(\underline{0}) \text{ (Twin A)}) \quad (4.19)$$

These matrix elements are clearly smaller than matrix elements between one-site excitons on the same sheet, and we have already seen that these are insignificant. Hence no new effects can be expected when the crystal twinning is taken into consideration. This conclusion, however, rests on the assumption that the wavefunctions of the sheets have cyclic boundary conditions. Because of the very limited extension of each sheet in the b-direction, it is conceivable that this assumption is not valid, and that another kind of wavefunctions must be found. But no conclusions can be drawn before the nature of the new boundary conditions is known.

The line at  $3212 \text{ \AA}$  might be assigned to the 0-0 molecular transition plus a lattice vibration. The broadness of the line could be due to a packet of vibrations of nearly equal frequencies or to the breakdown of the selection rule  $\Delta K = 0$  when lattice vibrations are excited. No investigation of lattice frequencies of crystalline decaborane has been reported, but heat capacity data below  $30^\circ \text{ K}$  (65) give a maximum Debye frequency of  $500 \text{ cm}^{-1}$ .

Concluding Remarks.--We have now succeeded in finding at least partial answers to the questions that were raised at the end of Chapter 1. Evidence is found for only one electronic transition of energy less than 5.0 eV, the energy of the 0-0 transition being 3.85 eV in the crystal. If there is another transition, it must be of only slightly higher energy so that it is concealed by the 3.85 eV transition.

The magnitude of the transition moment and the oscillator strength which were determined from the absorption spectrum of decaborane in cyclohexane, indicate that the transition is allowed, and this assumption was confirmed by a detailed analysis of the crystal spectrum which clearly showed that the excited state of the free molecule is a  $B_1$  or a  $B_2$  state. The transition is hence allowed for radiation polarized along the molecular x- or y-axis.

The magnitude of the crystal field induced splitting of vibronic levels was shown to be insignificant, so the lines observed in the crystal spectrum at  $4.2^\circ \text{ K}$  must be due to vibrations of the electronically excited molecule. Three frequencies,  $425 \text{ cm}^{-1}$ ,  $390 \text{ cm}^{-1}$ , and  $135 \text{ cm}^{-1}$ , are predominant, but since the gas phase spectrum lacks structure, they cannot be correlated with any frequencies of the molecule in the ground state.

Finally the solvent effect indicates that the dipole moment of the excited state is less than the dipole moment of the ground state.

## CHAPTER V

### CONCLUSIONS AND RECOMMENDATIONS

The absorption spectra in the near ultraviolet of decaborane gas, solutions and crystals were investigated, and one electronic absorption band with the 0-0 transition at  $3.81 \pm 0.06$  ev in solution in cyclohexane,  $3.86 \pm 0.03$  ev in the gas, and 3.85 ev in the crystal was found.

The existence of another excited electronic state of slightly higher energy cannot be ruled out however, as the absorption due to transitions to this state might be concealed by the absorption due to the 3.85 ev transition.

Assuming that the absorption of decaborane in cyclohexane is due to one transition only, the transition moment and oscillator strength are

$$p^2 = 0.21 \times 10^{-16} \text{ cm}^2 \quad \text{and} \quad f = 0.10$$

respectively.

The shift of the 0-0 transition towards the blue in polar solvents indicates that the dipole moment of the excited state is less than that of the ground state.

The wavefunction of the excited state of the free molecule is either of  $B_1$  or  $B_2$  symmetry, and the transition is hence allowed and polarized perpendicular to the two-fold symmetry axis of the molecule. In the crystal the electronic transition is accompanied by three totally symmetric boron framework vibrations of the excited molecule,

$$\nu_1 = 425 \text{ cm}^{-1}, \nu_2 = 390 \text{ cm}^{-1}, \text{ and } \nu_3 = 135 \text{ cm}^{-1}$$

A detailed discussion of the wavefunctions and energies of the optically active excited crystal states indicates that the Davydov-splitting should be too small to be observed under the experimental conditions, and indeed none was observed.

The lack of vibrational structure of the gas phase absorption spectrum and the increasing continuous background absorption in the crystal indicate dissociation in agreement with observations of other workers (66).

Since the energy of the O-O transition (3.85 eV) is considerably higher than the highest energy of the luminescence spectrum observed by Pimentel and Pitzer, we suggest that the luminescence is due to a lower-lying triplet state.

It is seen that all three models of bonding in decaborane described in Chapter I predict a symmetry of the excited state in agreement with our assignment, but there is no evidence for the second transition predicted by both the ECL and MLL model. The energy of the transition predicted from the MLL model is far too great, while the free particle in hemispherical box model is surprisingly accurate.

Both the ECL and the MLL model predict that the transition would decrease the charge density on boron atoms 2 and 4 and increase the charge density on boron atoms 5, 7, 8, and 10, which agrees with the observation that the dipole moment of the excited state is less than the dipole moment of the ground state.

It was found that the absorption spectrum of 2,4-diiododecaborane in acetonitrile exhibits two peaks, one at  $3130 \text{ \AA}$  and one at wavelengths

shorter than  $2300 \text{ \AA}$ . Work is presently going on in this laboratory to determine the symmetries of the two excited states in order to correlate them with the corresponding states in decaborane.

During recent years so many derivatives of decaborane have been synthesized and characterized that a critical comparison of their absorption spectra should yield considerable information.

## APPENDIX

### ON THE CHEMISTRY OF DECABORANE

Since they are not mentioned in the literature, brief note will be made of two observations on the chemistry of decaborane that were made accidentally during the course of this work:

Decaborane was found to react with acetone to form a white crystalline substance that could be sublimed at room temperature.

2,4-diiododecaborane reacts readily with acetonitrile at room temperature to form a substance characterized by a strong absorption peak at  $2450 \pm 30 \text{ \AA}$ .

No attempt was made to investigate the products.

## BIBLIOGRAPHY

1. Mm. Gay-Lussac et Thenard, "Notice. Sur la Decomposition et la Recomposition de l'Acide Boracique," Annales de Chimie **68**, 169 (1808).
2. Francis Jones and R. L. Taylor, "On Boron Hydride," Journal of the Chemical Society (London) **39**, 213 (1881).
3. William Ramsay and H. S. Hatfield, "Preliminary Note on Hydrides of Boron," Proceedings of the Chemical Society (London) **17**, 152 (1901).
4. Alfred Stock, Hydrides of Boron and Silicon, Ithaca: Cornell University Press, 1933.
5. Richard E. Dickerson, Peter S. Wheatley, Peter A. Howell, William N. Lipscomb, and Riley Schaeffer, "Boron Arrangement in a B<sub>9</sub> Hydride," The Journal of Chemical Physics **25**, 606 (1956).
6. H. G. Heal, Recent Studies in Boron Chemistry, London: The Royal Institute of Chemistry, 1960.
7. Stock, op. cit., pp. 153 ff.
8. W. C. Price, "The Absorption Spectrum of Diborane," The Journal of Chemical Physics, **16**, 894 (1948).
9. J. S. Kasper, C. M. Lucht, and D. Harker, "The Crystal Structure of Decaborane, B<sub>10</sub>H<sub>14</sub>," Acta Crystallographica **3**, 436 (1950).
10. Emmett B. Moore, Jr., Richard E. Dickerson and William N. Lipscomb, "Least Squares Refinements of B<sub>10</sub>H<sub>14</sub>, B<sub>4</sub>H<sub>10</sub> and B<sub>5</sub>H<sub>11</sub>," The Journal of Chemical Physics **27**, 209 (1957).
11. Gloria Silbiger and H. S. Bauer, "The Structures of Hydrides of Boron. VIII. Decaborane," The Journal of the American Chemical Society **70**, 115 (1948).
12. Charles M. Lucht, "An Analysis of the Electron Diffraction Data for Decaborane," The Journal of the American Chemical Society **73**, 2373 (1951)
13. A. W. Laubengayer and R. Bottei, "The Dipole Moment of Decaborane," The Journal of the American Chemical Society **74**, 1618 (1952).



14. Riley Schaeffer, James N. Shoolery, and Robert Jones, "Nuclear Magnetic Resonance Spectra of Boranes," The Journal of the American Chemical Society **79**, 4606 (1957).
15. R. E. Williams and I. Shapiro, "Reinterpretation of Nuclear Magnetic Resonance Spectra of Decaborane," The Journal of Chemical Physics **29**, 677 (1958).
16. N. J. Blay, J. Williams, and R. L. Williams, "Boron Hydride Derivatives. Part II. The Separation and Identification of Some Ethylated Pentaboranes and Decaboranes," Journal of the Chemical Society (London) **1960**, 424 (1960).

N. J. Blay, I. Dunstan, and R. L. Williams, "Boron Hydride Derivatives. Part III. Electrophilic Substitution in Pentaborane and Decaborane," Journal of the Chemical Society (London) **1960**, 430 (1960).

R. L. Williams, I. Dunstan, and N. J. Blay, "Boron Hydride Derivatives. Part IV. Friedel-Craft Methylation of Decaborane," Journal of the Chemical Society (London) **1960**, (1960).

I. Dunstan, R. L. Williams, and N. J. Blay, "Boron Hydride Derivatives. Part V. Nucleophilic Substitution in Decaborane," Journal of the Chemical Society (London) **1960**, 5012 (1960).

I. Dunstan, N. J. Blay, and R. L. Williams, "Boron Hydride Derivatives. Part VI. Decaborane Grignard Reagent," Journal of the Chemical Society (London) **1960**, 5016 (1960).
17. Manny Hillman, "The Chemistry of Decaborane. Iodination Studies," The Journal of the American Chemical Society **82**, 1096 (1960).
18. I. Shapiro, Max Lustig, and Robert E. Williams, "Exchange Sites in the Deuteration of Decaborane," The Journal of the American Chemical Society **81**, 838 (1959).
19. John A. Dupont and M. Frederick Hawthorne, "Deuterium Exchange of Decaborane with Deuterium Chloride under Electrophilic Conditions," The Journal of the American Chemical Society **81**, 4998 (1959).
20. Riley Schaeffer, "A New Type of Substituted Borane," The Journal of the American Chemical Society **79**, 1006 (1957).
21. Josina van der Maas Reddy and William N. Lipscomb, "Molecular Structure of  $B_{10}H_{12}(CH_3CN)_2$ ," The Journal of Chemical Physics **31**, 610 (1959).
22. M. Frederick Hawthorne and Anthony R. Pitochelli, "Displacement Reactions on the  $B_{10}H_{12}$  Unit," The Journal of the American Chemical Society **80**, 6685 (1958).

23. W. E. Keller and H. L. Johnston, "A Note on the Vibrational Frequencies and the Entropy of Decaborane," The Journal of Chemical Physics **20**, 1749 (1952).
24. L. J. Bellamy, W. Gerrard, M. F. Lappert, and R. L. Williams, "Infrared Spectra of Boron Compounds," Journal of the Chemical Society (London) **1958**, 2412 (1958).
25. George C. Pimentel and Kenneth S. Pitzer, "The Ultraviolet Absorption and Luminescence of Decaborane," The Journal of Chemical Physics **17**, 882 (1949).
26. John L. Margrave, "Ionization Potentials of  $B_5H_9$ ,  $B_5H_8I$ ,  $B_{10}H_{14}$ , and  $B_{10}H_{13}C_2H_5$  from Electron Impact Studies," The Journal of Chemical Physics **32**, 1889 (1960).
27. Masatoshi Yamazaki, "Electronic Structure of Diborane," The Journal of Chemical Physics **27**, 1401 (1957).
28. W. C. Hamilton, "A Molecular Orbital Treatment of Diborane as a Four-Centre, Four-Electron Problem," Proceedings of the Royal Society of London A **235**, 393 (1956).
29. H. I. Schlessinger and A. B. Burg, "Recent Developments in the Chemistry of Boron Hydrides," Chemical Reviews **31**, 1 (1942).
30. Walter C. Hamilton, "On the Electronic Structure of Diborane," The Journal of Chemical Physics **29**, 460 (1958).
31. W. H. Eberhardt, Bryce Crawford, Jr., and William N. Lipscomb, "The Valence Structure of the Boron Hydrides," The Journal of Chemical Physics **22**, 989 (1954).
32. Emmett B. Moore, Jr., L. L. Lohr, Jr., and William N. Lipscomb, Private Communication. To be published.
33. Pimentel and Pitzer, op. cit., p. 883
34. Dr. A. E. Newkirk, Private Communication.
35. Heal, op. cit., p. 9.
36. Hillman, op. cit., p. 1096.
37. M. Frederick Hawthorne, Anthony R. Pitochelli, R. Donald Stramm, and John J. Miller, "The Preparation and Characterization of Salts Which Contain the  $B_{10}H_{13}$  Anion," The Journal of the American Chemical Society **82**, 1825 (1960).
38. Riley Schaeffer, op. cit., p. 1006.

39. Eastman Kodak Company, Materials for Spectrum Analysis, 2nd Ed., Eastman Kodak Company, 1954.
40. George T. Furukawa and Rita P. Park, "Heat Capacity, Heats of Fusion and Vaporization, and Vapor Pressure of Decaborane ( $B_{10}H_{14}$ )," Journal of Research of the National Bureau of Standards **55**, 255 (1955).
41. Ibid., p. 255.
42. William George Trawick, The Polarized Ultraviolet Absorption Spectra of Single Crystals of Polyatomic Substances at Low Temperature, Ph.D. Thesis, Georgia Institute of Technology, 1954.
43. Russell B. Scott, Cryogenic Engineering, Princeton: D. Van Nostrand Company, Inc., 1959, p. 277 and p. 307.
44. L. J. Schoen, L. E. Kuentzel, and H. P. Broida, "Glass Dewars for Optical Studies at Low Temperatures," The Review of Scientific Instruments **29**, 633 (1958).
45. William H. Duerig and Irving L. Mador, "An Optical Cell for Use with Liquid Helium," The Review of Scientific Instruments **23**, 421 (1952).
46. John Strong, Procedures in Experimental Physics, New York: Prentice Hall, Inc., 1939, p. 157.
47. Ibid., p. 154
48. S. Davydov, "Theory of Absorption Spectra of Molecular Crystals," Journal of Experimental and Theoretical Physics (U.S.S.R.) **18**, 210 (1948). Translated by M. Kasha and distributed under Contract N6-ori-211, T.O. 3, Office of Naval Research.
49. Harvey Winston and Ralph S. Halford, "Motions of Molecules in Condensed Systems: V. Classification of Motions and Selection Rules for Spectra According to Space Symmetry," The Journal of Chemical Physics **17**, 607 (1949).
50. Harvey Winston, "Electronic Energy Levels of Molecular Crystals," The Journal of Chemical Physics **19**, 156 (1951).
51. G. F. Koster, "Space Groups and Their Representations," Solid State Physics **5**, 174 (1957).
52. Donald S. McClure, "Electronic Spectra of Molecules and Ions in Crystals, Part I. Molecular Crystals," Solid State Physics **8**, 1 (1959).
53. Koster, op. cit., p. 177.

54. Walter Ledermann, Introduction to the Theory of Finite Groups, 3rd. ed. Edinburgh: Oliver and Boyd, 1957, p. 102.
55. Koster, op. cit., p. 214 ff.
56. William I. Simpson and Don L. Peterson, "Coupling Strength for Resonance Force Transfer of Electronic Energy in van der Waals Solids," The Journal of Chemical Physics 26, 588 (1957).
57. Pimentel and Pitzer, op. cit., p. 882.
58. Keller and Johnston, op. cit., p. 1749.
59. Kasper, Lucht, and Harker, op. cit., p. 436.
60. The International Union of Crystallography, International Tables for X-Ray Crystallography, Birmingham: The International Union of Crystallography, 1952, p. 96.
61. Ibid., p. 96.
62. H. Sponer and E. Teller, "Electronic Spectra of Polyatomic Molecules," Reviews of Modern Physics 13, 75 (1941).
63. David Fox and Otto Schnepp, "Theory of the Lower Excited Electronic States of the Benzene Crystal," The Journal of Chemical Physics 23, 767 (1955).
64. Kasper, Lucht, and Harker, op. cit., p. 449.
65. Eugene C. Kerr, Nathan C. Hallett, and Herrick L. Johnston, "Low Temperature Heat Capacity of Inorganic Solids. VI. The Heat Capacity of Decaborane,  $B_{10}H_{14}$ , from 14 to 305° K," The Journal of the American Chemical Society 73, 1117 (1951).
66. Keller and Johnston, op. cit., p. 1749.

## VITA

Arne Haaland was born on February 15, 1936 in Drammen, Norway to Anna Solveig and Reidar Haaland. He graduated from high school (Drammens Latinskole) in June 1954, and after having worked for a year he entered the Norwegian Institute of Technology in Trondheim, Norway to study chemical engineering. At the end of the sophomore year he went to Georgia Institute of Technology for a year's study under the World Student Fund program, and at the end of the first year there he was admitted to the graduate division in May 1958 and began working towards a doctorate in chemistry.

In October 1961 he will enter the Royal Norwegian Air Force to serve for 18 months.